# MICROSCALE PRECISE POSITION MEASUREMENT AND MONITORING OF SLIDING VALVES

**A Thesis submitted to**
**the Graduate School of Engineering and Science of**
**İzmir Institute of Technology**
**in Partial Fulfillment of the Requirements for the Degree of**

**MASTER OF SCIENCE**

**in Mechanical Engineering**

**by**
**Önder Mahir TANRIYAPISI**

**December 2019**
**İZMİR**

# ACKNOWLEDGMENTS

I would like to begin by thanking Serhan ÖZDEMİR, my esteemed supervisor, for his continuous patience, encouragement and assistance. I could not have concluded this study without his understanding, support, and knowledge. I would also like to thank Assoc. Prof. M. İ. Can DEDE and Assoc. Prof. Pınar DEMİRCİOĞLU for their valuable time.

I would like to express my thanks for the support of my dear and respected Delphi Technologies colleagues during my thesis. For their understanding and help, I'll always be grateful.

Last but not the least, I want to thank my precious family who, in every step I have taken, have helped me throughout my life.

# ABSTRACT


## MICROSCALE PRECISE POSITION MEASUREMENT AND MONITORING OF SLIDING VALVES

In present study, a sensor, Accuciser, is presented to know the position of sliding valves which have ferromagnetic or diamagnetic guide. The main objective is to develop a sensor, which has low cost and high resolution, that measures the displacement of engine valves or SCR injectors which are used in especially in the automotive industry. For now, the position of the valves, which are using in propulsion systems, or SCR injector cannot be known with a signal from an analog sensor. Instead of analog sensor, the mapping is used from experimental data. However, this mapping gives inaccurate results due to driving style or usage of the system. After seeing the gap in these systems, the sensor was developed, and it fulfils this gap. The sensor is developed based on Faraday's Law of Induction which was discovered by Michael Faraday in 1830. The sensor consists of two coils and one coil located on top of the other. The most important property of the proposed sensor is working with a direct current. In fact, if the valve is actuated by an electromagnetic force, there is no power consumption on the sensor. The experimental results, for the latter property, are corroborated by theoretical calculations. The output of the sensor is directly proportional to the displacement of the core and it has high signal-to-noise ratio because of the nature of magnetism. The results show that using Accuciser, the proposed sensor, to monitor valve displacement gives more reliable results than current technology.



*Keywords and Phrases*: Electromagnetic, Electromagnetic interaction, Valve, Precise Position Measurement, Inductive Measurement, Magnetism

# ÖZET

## KAYAR VALFLERİN MİKRO ÖLÇEKTE HASSAS POZİSYON ÖLÇÜMÜ VE İZLENMESİ

Bu çalışmada, ferromanyetik ve/veya diyamanyetik klavuza sahip olan kayar valflerin pozisyonunu okuyabilmek için bir sensör geliştirilmiştir. Temel amaç, özellikle otomotiv sektöründe kullanılan motor sübapları veya SCR enjektörü gibi komponentlerin pozisyonlarının anlık olarak gözlemlenebilmesi için gerekli olan düşük maliyetli ve yüksek çözünürlüklü bir sensör geliştirilmesidir. Hali hazırda yakıt sisteminde veya seçici katalitik indirgemede kullanılan enjektörlerin ve valflerin pozisyonları analog bir sensörden alınan bilgilere göre bilinememektedir. Bunun yerine deneylerden alınan verilere göre bir haritalama yapılmaktadır. Ancak aracın veya sistemin kullanıma bağlı olarak bu haritalama yanlış sonuçlar verebilmektedir. Sistemdeki bu açığın görülmesiyle yeni bir sensöre ihtiyaç duyulmuştur ve prototipi yapılan sensör ile bu açık giderilmiştir. Dizayn edilen sensör, Michael Faraday trafından 1830 yılında bulunan Faraday'ın indüksiyon kanunu baz alınarak geliştirilmiştir. Sensör üst üste sarılmış iki adet bobinden oluşmaktadır. Sensörün en önemli özelliklerinden birisi doğru akımla çalışmasıdır. Hatta kullanılan valf elektro manyetik tahrik ile çalışıyor ise, sesörde güç tüketimi olmamaktadır. Teorik hesaplamalar ile desteklenen deney sonuçları sensörün bu özelliğini kanıtlamaktadır. Sensörden alınan çıkış sinyali valfin yer değiştirmesiyle doğru orantılı olup manyetizmanın doğası gereği yok denebilecek kadar az bir gürültüye sahiptir. Sonuçlar göz önünde bulundurulduğunda ve günümüz teknolojisi ile kıyaslandığında, Accuciser sensörü daha güvenilir sonuçlar vermektedir.

*Anahtar Kelimeler ve İfadeler*: Elektromanyetik, Elektromanyetik etkileşmeler, Valf, Hassas Pozisyon Ölçümü, Endüktif Ölçüm, Manyetizma

# TABLE OF CONTENTS

# LIST OF FIGURES

**Figure** **Page**

**Figure** **Page**

# LIST OF TABLES

**Table** **Page**

# LIST OF SYMBOLS

| | | |
|---|---|---|
| $f$ | Frequency | 1/s |
| B | Magnetic field | Tesla |
| S | Area | $m^2$ |
| L | Inductance | Henry |
| I, i | Current | A |
| r | Radius | m |
| $l$ | Magnetic circuit length | m |
| $\rho_v$ | Electric charge density | $C/m^3$ |
| D | Electric flux density | $C/m^2$ |
| $J$ | Electric current density | $A/m^2$ |
| E | Electromotive force | Volts |
| t | Time | s |

**Greek Letters**

| | | |
|---|---|---|
| $\delta$ | Skin depth | m |
| $\mu$ | Magnetic permeability | H/m |
| $\sigma$ | Electrical conductivity | 1/ohms m |
| $\Phi$ | Magnetic flux | Wb |
| $\varepsilon$ | Electromotive force | Volts |

# CHAPTER 1

# INTRODUCTION

## 1.1. Literature Review

Within the last few decades, there have been a growing need and a push for sub-micron position measurements for mechanical systems in general. Even though this level of accuracy has been achieved earlier for some other engineering fields, such as electronics, this is relatively new in mechanical engineering measurements. Accurate displacement sensing is vital in many feedback control systems. It is not uncommon for a precision mechanical system whose stroke is half a millimeter, and it is intended to be measured with 10bit resolution.

In 2012, Suresh and Ramu were working on real time measurement of position with LVDT. They also identified direction from their modified LVDT. Conventional LVDTs and modified LVDT were compared in this work. In conventional LVDTs, direction of the core is detected by phase detector circuit. However, Suresh and Ramu made an LVDT which detect the direction of the core by observing of the sign (Suresh & Ramu, 2012).

In Suresh and Ramu's design, direction of winding of secondary windings are the same. After modifying LVDT sensor, they implemented transformers to amplify the electrical signal, then, with the diode bridges, AC/DC conversion was made. Finally, the signals can easily be read with simple multimeters. Specifications of the sensor are given below;

Table 1. Specifications of LVDT which was design (Suresh & Ramu, 2012)

| | |
|---|---|
| Inner diameter of the shell | 16.6 mm |
| Outer diameter of the shell | 17.0 mm |
| Diameter of the copper wire | 0.315 mm |
| Diameter of the core | 15.0 mm |
| Material of the core | Iron |

Blejan et al., published a paper in 2016 which is about smart position and transducer. In this work, they developed an LVDT for measuring speed and position. The LVDT and the measuring amplifier system were tested on hydraulic damper for rail wagons. They built the LVDT in classical structure which is half bridge inductive and three wire connections. The useful signal was processed with synchronous demodulation method. This method was also combined with ratiometric algorithm which is the division of the magnitude of difference an summation of the signal samples at 90 degree respectively 270 degree phase shift in reference to power signal (Blejan, Ilie, & Drumea, 2016).

In 2015, Cheng-Wei Pei focused on signal conditioning of LVDT. There are two distinct ways for conditioning LVDT output signals which are analog and digital conditioning. Pei worked on analog conditioning in his works. Demodulation and lowpass filtering of output signal of LVDT are run-of-the-mill method. On the other hand, the precision of demodulating is highly sensitive to phase adjustment. Furthermore, in this work, Pei mentioned that there are some problems in demodulation method, such as; time jitter and charge injection due to demodulation of signal. Therefore, the main idea is to change the form of signal from RMS to DC in this work. It was done by LTC1967 RMS to DC converter integrated circuit. This IC provides 0.15% linearity error and 0.3% gain error. Pei used a separate circuit for phase detection to find out direction of the movement.

Schaevitz E-100 with plus or minus 2.5mm linear range was used in this work. Excitation frequency of LVDT, recommended from company, is up to 10kHz. In the output of the circuitry there existed LT1807 op-amp. While one half of LT1807 used for biasing the sine wave output of the LVDT, the other half used for buffering LVDT output for good signal condition. Then the output of LT1807 was converted to DC by LTC1967. Output DC signal of the LTC1967 was proportional to the displacement of the LVDT core (Dobkin, Hamburger, & Pei, 2015).

Drumea et al. worked on system on chip signal conditioner of for LVDT sensors in 2006. They use MSP430F149 microcontroller to process the output signal. This microcontroller involves all peripherals for signal conditioning of LVDT. Such as; analog-digital converter, timers PWM modules etc. They focused on control application of electro-hydraulic system. Position adjusting is common industrial control system. They used LVDT sensor which are manufactured by Research Institute for Hydraulics and Pneumatics (Drumea, Vasile, Comes, & Blejan, 2006).

Drumea et al. used three operational amplifiers and one comparator on the analog side an MSP430F149 microcontroller on the digital side while signal conditioning of the LVDT output signal. The reasons for using amplifiers were that one of the amplifiers was used as adapter and the other two were used as drivers which were energizing the coils, because MCU can't provide currents required by coils. The main element of this work was MSP430F149. Because it measures the voltage difference and calculate the displacement value and two pins for DAC, output driver and serial communication. The microcontroller is driven with low frequency crystal which is at 32768Hz. The low frequency has some advantages which are reduced electromagnetic interference emissions low power etc. Primary coil of the LVDT was excited with square signal which has the magnitude of 3V peak to peak and 5kHz frequency. The output signal was converted to 16 bits digital value (Drumea et al., 2006).

Korkmaz, H and Can, B. used LVDT in thermal expansion of materials. In this work, they used dilatometry technique to measure displacement under controlled temperature. Dilatometry is that sample is connected to negligible load and under this circumstance temperature is changed, then displacement of material is measured. To measure displacement there was used LIN156 LVDT. The reason for using this model of LVDT is that the core of LIN156 can freely move both side (some of the models have spring loaded core). For the signal conditioning, there was used S7AC signal conditioner (Korkmaz & Can, 2003).

The LVDT was connected and contacted with ceramic push-rod mechanism to metal sample, because furnace would reach up to 600 centigrade. Therefore, LVDT needs to be isolated from this elevated temperature. The integration of LVDT is important in this work, since armature of transducer must leave 40mm away from the sample after clamping LVDT. Normally, in this situation zero output signal produced. However, in this work, at that point, 5V output is produced. This can be made by adjusting S7AC circuit. This condition module is used for transducers which require synchronous demodulation and AC excitation signal and producing DC output current or voltage. To get voltage and displacement change curve, simple setup was built by Korkmaz and Can. They used a micrometer which has 100 turns for 1mm, and it is connected to armature. Then voltage data was collected and reached the curve (Korkmaz & Can, 2003).

Masi et al., built up a high precision radiation tolerant LVDT conditioning module. The reason to make a radiation-tolerant conditioning module is that this project was a part of CERN and radiation is a problem in there. Masi et al. compare analog

synchronous demodulation circuits and components and their design. There are several ICs for analog techniques. For instance, SE5521, from Philips Semiconductors, works based on demodulation technique and phase of the output signal from LVDT. In this situation, cable length, which is driving the transducer, is very important. Because long cable means that until output signal reaches the conditioning circuit, message signal is exposed to noise and disturbance from the environment. This means that impedance seen by the circuitry transforms inductive to capacitive and it is challenging to make phase recovery also expensive. The other components are AD698 and AD598. These ICS works based on ratiometric algorithm. First one divides output signal by input excitation signal. Thus, this component is also phase sensitive. Latter makes also division, but it divides difference of two secondary signal by summation of them. The sum of the secondary voltage must stay constant with the stroke length and also noise immunity of this method is not better than the synchronous demodulation technique. In the light of these, Masi et al. chose a three-parameter sine-fit algorithm to regenerate the output signal of LVDT and ratiometric algorithm to read the exact position of the core. These techniques allows them to tune the device locally and read the position of the core with aa accuracy of a few micrometers even low-signal-to noise ratio (Masi et al., 2014).

Masi et al used FPGA (Field Programmable Gate Array) to generate input signal for primary coil of LVDT. This synthesized signal is sent to digital to analog converter. In addition, FPGA makes signal conditioning. Both algorithms were embedded to FPGA. The sensitivity of the signal conditioner module depends on electronics and sensor temperature. Therefore, they used Schaevitz HCA3000 LVDT, this LVDT is also rugged to radiation. The LVDT has a full stroke length of 80mm. After experiments, it was observed that, uncertainty of the LVDT is always below 300nm. The conditioning module has nearly 45nm/C position drift after room temperature of 25C degree. They said that, for the radioactive environment, standard LVDT signal conditioning modules are not effective and sufficient (Masi et al., 2014).

There are numerous of examples for sliding valves. The most commonly known sliding valves in the automotive industry are intake or exhaust valve of an engine, diesel or gasoline injectors, DEF (Diesel Exhaust Fluid) injectors, SCR (Selective Catalytic Reduction) valves which are using sliding valves etc.

When the calendars showed 2007, Coppo, M. et al. published a work that introduces (Coppo, Dongiovanni, & Negri, 2007). This linear optical displacement sensor was developed to address the difficulties in electromagnetic interference relating to the

sensitivity of traditional transducers when calculating the needle lift in the Diesel-powered fuel injectors. A laser-light emitter, a receiver and a device were installed in the sensor to modulate the light intensity reaching the receiver according to the position of the moving element of the injector. Thereby the injector body had two rectangular windows, whereas the third window was strongly linked and aligned with the fixed piston, so as to achieve a clearing zone that varied linearly with the needle position.

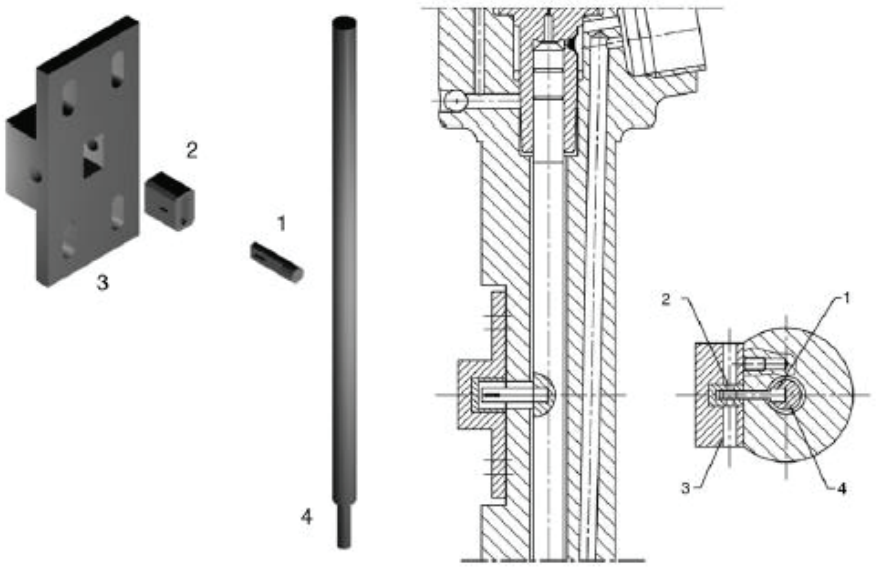


Figure 1. Mounting of the sensor to the injector body (Source: Coppo et al., 2007)

In Figure 1, Pin 1 is fitted to the control piston with one of the above-mentioned optical windows. Upon mounting the sensor, the pin is inserted into a slotted cap 2 in which both other windows are machined. The cap is connected to the injector body and keeps in place Element 3 and provides two-hole connections to the optical fibrous cables and four holes, which are able to fit elements 2 and 3 with screws on the injector body and to fix their position in relation to pin 1 (Coppo et al., 2007).

However, as can be understood from the design, it has some disadvantages. First of all, it can be applied only in lab environment. The reason is that NHB (nozzle holder body) is thinned to put apparatus onto body. This application cannot be used on the injector on working engine. The other problem is fluid flow. The sensor is an optical sensor and therefore the flow may affect the resolution and accuracy of the sensor.

In 2013, Amirante et. al.(Amirante, Catalano, & Coratella, 2013), proposed a new technique to measure the displacement of a CRDI (Common Rail Diesel Injector) to

improve fuel consumption and efficiency. This technique shows how a new cheaper sensor should be developed for a reliable needle lift calculation, as an additional step within the scope of a wider project aimed at increasing the rate of Diesel injection optimization. The proposed transducer is based on a simple and cheaper model that incorporates a reliable solution to the needle elevation problem (Amirante et al., 2013). Optical systems are chosen for considerable skills, including to assess the shift of the control piston in a CR injection unit, in order to ensure high levels of signal cleanliness in the measurement applications (Amirante et al., 2013). In the figure below, the invented technique can easily be seen:

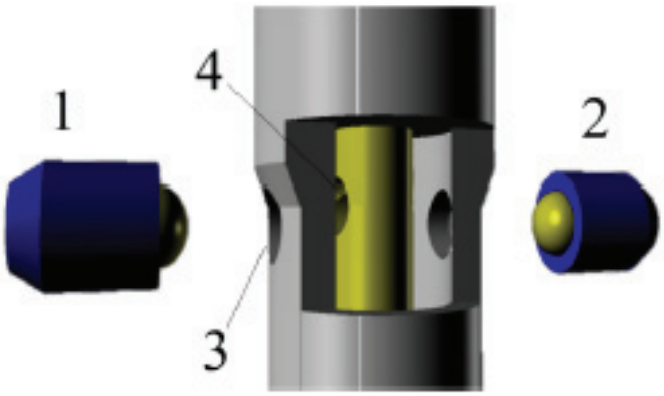


Figure 2. Optical sensor for a needle position sensing (Source: Amirante et al., 2013)

Number 1 in Figure 2 indicates the diode emitter of infrared light while number 2 indicates photo receiver. Number 3 and number 4 show the holes on the body of injector and the needle of an injector respectively (Amirante et al., 2013). Even in the presence of powerful electro-magnetic fields, the sensor demonstrates great repeatability and precision, thanks to its light beam transmission concept. In addition, its cost is worth highlighting, which is significantly lower than the transducer for eddy currents, which is some thousand euros.

However, there are some problems for that sensor. One of them is drilling the injector body and control piston. The CRD injectors are working on 2200 bars at maximum performance. Under these pressures, it is not a wise choice to drill the body and control piston. Furthermore, it is not applicable in industry. The reason is that there are many cables going out from the injector body, and this will cause design issues. The other issue is the fluid flow in the body part as previous design which belongs to Amirante

et al. When fluid flows in front of the linear optical sensor, the light will refract, and this will cause accuracy and resolution problems.

The principal source of propulsion for vehicles has long been internal combustion engines. The continuing demand for reductions in transport-related emissions leads to an ongoing pursuit of fuel economy improvements. This pushes producers to look for new ways to improve efficiency. The gas exchange system is one of the main areas of focus for the ICE. The inlet of the induction air and outlet of exhausts is governed by poppet valves and camshafts are performed in almost all ICEs. The inherent sync with piston movement is one of the reasons for its popularity. It assumes, however, that only certain motor speeds and loads can be optimized and that significant increases in output can be achieved when valve timing can be varied. Variable valve timing (VVT) on camshaft can be used, but due to its mechanic and therefore its non-variable nature, these systems are limited. In addition, these systems do not generally allow variable valve lifting, variable valve timing only. Another way to get rid of the camshaft is to control a full-varying valvetrain (FVVT), which is also adjustable for each valve and combustion cycle, by using pneumatics or hydraulic valves. Over the past decade, the researchers would like to further optimize engine performance across the entire operating range by using a fully adjustable lift, duration and time-based electronic controlled pneumatic / hydraulic valve actuator system.

In a camless FVVT, in terms of the opening and closing times of valves and the valve lift, there is infinite flexibility that valve is operated by a separate actuator, so that each valve can be freely activated. It provides many possibilities of optimization for the exchange of fuel, combustion and a wide range of new concepts. Many FVVT solutions are available, such as variable camshafts, hydraulics, electromagnetic and pneumatic actuation. Such structures have all their own advantages and disadvantages (Gundersen, 2009). VVT offers a variety of benefits and advantages. The increased couple of things VVT can make possible are increasing torque, higher efficiency, lower energy usage, and advanced combustion concepts.

R.J. Osborne and others have studied different FVVT concepts and compare them with other types of valve timing and lifting systems (Osborne, Stokes, Lake, Carden, & Mullineux, 2018). According to Osborne et al., Due to no energy recovery, EPVA suffers from high energy consumption. The excess air, still at high pressure, is only wasted into the atmosphere. Spring force is used once the cam rolls off the valve with a camshaft operation. The FVVT's use of expansion rather than input air is beneficial, but it still

consumes quite a plethora of energy. In fact, the highest of all the concepts investigated (Osborne et al., 2018). The other drawback which was reported by Osborne et al. is the engine architecture changes. To remove the camshaft completely and replace it with FVVT actuators obviously requires improvements to the engine design, even if these are minor but the same as similar systems (Osborne et al., 2018). The noise also one of the disadvantages of FVVTs. However, this was reported as a medium drawback of FVVTs (Osborne et al., 2018). The reason is that the one can adjust the seating velocity and so the seating noise can be reduced (Osborne et al., 2018).

For decades, techniques for the variable valve actuator (VVA) have been suggested to improve performance and efficiency during emission controls. A full investigation and experimental analysis have been performed of the advantages of engine performance for specific valve actuation methods, such as Early Intake Valve Closing (EIVC), Late Intake Valve Closing (LIVC) and Variable Max Valve Lifting (Sellnau & Rask, 2003). Such techniques include the disabling of valves, independent, continuously variable cam profiling and finally camless engineering such as electro-hydraulic and electromagnetic drive. Despite the performance advantages, VVA is, however, not taken advantage of in most current internal combustion engines. Extensions of traditional cam technologies are included (Sellnau & Rask, 2003).

In 2006, the new type of Fully Flexible Valve actuator was proposed for engine valves (Cope & Wright, 2006). This research focused primarily on the development, installation and testing of the completely flexible electromagnetic valve actuator. The development process included a number of modifications, moving magnets, coils and/or a plunger. In terms of dynamic efficiency, the selected prototype worked far better than other models and had desirable features such as stationary magnets and a stationary coil (Cope & Wright, 2006). Acceleration per square root of dissipated power was described as dynamic efficiency by Cope and Wright.

In order to forecast the valve output under various conditions, in particular various acceleration profiles, dynamic simulation was developed. Interference with the valve piston can be avoided in modes of failure. In the light of these simulations, Cope and Wright concluded that the results indicate the actuator has its inherent advantages, like variable timing, variable lift and low valve landing speed, in a totally flexible valve actuator (Cope & Wright, 2006).

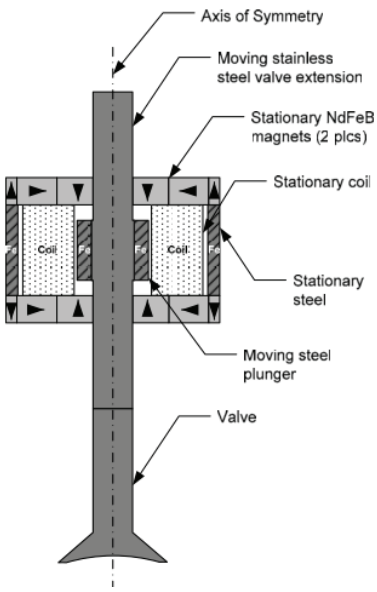


Figure 3. Actuator design for free valve mechanism (Source: Cope & Wright, 2006)

In the light of above discussions, it can be easily seen that a displacement sensor is needed to know the exact position of the inlet valve of an engine, or the needle position of any type of injector. In this thesis the electromagnetic based displacement transducer is developed. The starting point of design was LVDT. However, while development of LVDT, it was investigated that if the housing is ferromagnetic or metal, LVDT is useless. The reason is the skin effect. Skin effect phenomenon indicates that if the frequency of the current is increasing, the magnetic field that penetrates through the wall thickness of the housing will decrease. The formula can be seen below:

$$\delta = \sqrt{\frac{2}{f\mu\sigma}} \tag{1.1}$$

δ is indicating the skin depth, while σ is indicating electrical conductivity of the housing material. $f$ is the frequency of the current which creates time varying magnetic field, and μ is magnetic permeability of the housing material.

If the materials that are using in automotive industry is considered it will not be a wise choice to use LVDT type displacement sensor with metal housing sliding valves. On this point the research was stuck. After detailed research, the way that how to overcome this skin effect and transfer the magnetic field to the medium of the housing was found.

A sensor model was introduced that tracks the existence of ferromagnetic bodies which travel inside steel pipes, by Popov, A. P. and Chugulev, A. O. in 2012 (Popov & Chugulev, 2012). This article presented a sensor that controls the presence of ferromagnetic metal objects in homogenous, non-magnetic, steel pipeline moving media with a strong electromagnetic field screening effect. The sensor has two parts which are primary winding and secondary winding. Primary winding is known as direct magnetizing current winding which is located on the outer part of the system. The secondary winding can be found between the housing (or steel pipe in Popov and Chugulev's work) and the primary winding (Popov & Chugulev, 2012). As shown in Figure 4, pipeline needs to be thinned to overcome saturation issue easily.

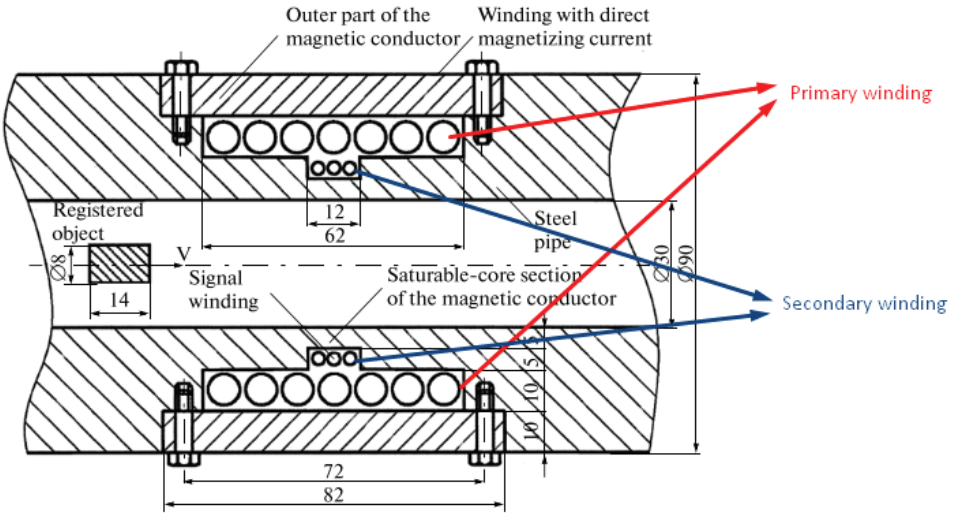


Figure 4. Steel pipe and sensor system to detect the ferromagnetic bodies in steel pipeline (Source: Popov & Chugulev, 2012)

Popov and Chugulev used the magnetic saturation phenomenon. Due to deep magnetic saturation of the pipe part with direct magnetizing current in the area of signal winding, the screening effect of the steel pipe is reduced many times in the proposed unit. It allows the identification, without using alternative magnetizing current, of ferromagnetic objects moving within the internal pipe cavity. The method of detection is based on the change in the magnetic flux that passes through the sensor signal winding on the saturable core section of the tube. The change of flow caused by ferromagnetic body entry into the area of the magnetic field of the inner cavity of the pipe also leads to

an electromotive force being produced throughout signal winding (Popov & Chugulev, 2012).

As mentioned before, there is no way to know that where is the needle of any type of injector or valve via signal from an analog sensor. Hopefully this thesis will be the solution of this problem. In Chapter 2 and Chapter 3, theory and methods which are used to develop this thesis will be shown. In Chapter 4, the design criteria and experiments can be seen for the proposed solution. After dead end was found with an LVDT because of skin effect phenomenon, this design was the inspiration for creating the sensor which is proposed in this thesis and named as “Accuciser”. The fundamental theory on the sensor is Faraday’s Law of Induction and the law is explicated in Chapter 2. The sensor properties are explained in Chapter 4.

# CHAPTER 2

# THEORY AND METHODS

## 2.1. History of Electromagnetism

The term “magnetism” was christened and the magnetic properties of natural ferric ferrite ($Fe_3O_4$) stones (lodestones) were described by Greek philosophers and in 600 B.C. Tales who is a great Greek philosopher, made the first observation on electrostatics. Actually, magnetism was coming from the word “magnesia” which is the name of the city near Aydın, in the time of ancient Greek. In the same century, Aristophanes discovered peculiar property of ambers. When he rubbed amber a piece of fur, amber gained a property of attracting some small materials such as feathers. For nearly 2000 years this fact covers its mystery. In 1600 AD Dr. William Gilbert investigated the behavior of amber and magnets. He was the first man who is used the word “electric” in his report which is about theory of magnetism(Ulaby & Ravaioli, 2014).

After the progress in 1600 AD, the development in electric and magnetic theory have become faster. In 1745 the first capacitor was invented by Leyden Jar. After Gilbert discover that force created by electric charges is a conclusion of a friction of distinct materials, Benjamin Franklin said electric forces are dipole and one is attractive and the other is repulsive. At the same time, William Watson, British scientist, reached the same results. At the beginning of the $19^{th}$ century, Alessandro Volta, Italian scientist, invented the first electric battery. After this invention, it was seen that electricity can be flow like a water in a pipe, rather than discharging itself by single spark or shock. In the light of this improvement, Volta shows that the electricity can be travel from one place to another by wire, hereby it was regarded as a significant improvement in the science of electricity. In 1820, the relationship between electric current and magnetism was discovered by Hans Christian Oersted. He discovered that a current carrying wire changes the direction of a needle of compass, and it indicates that a magnetic field can be produced by electric current. At the same time, Andre Marie Ampere, a French mathematician, explained the

electrodynamic theory for the first time. He indicated that two current carrying wires attracted and opposed each other while current flows same direction and opposite direction, respectively. He made mathematical explanation for this phenomenon, and the laws that govern the electric current and magnetic field. As a result of this unit of electric current became A, which is derived from his name. After these discoveries and inventions, Georg Simon Ohm, who is the German Physicist, delve into Volta's principle battery and Ampere's relationship of currents in circuit. In this investigation, he realized that there exists a heat in a circuit when there is a current and the amount of heat depends on the material that current flows in. Also, he discovered that if the potential difference remains constant, amount of current will proportionally change from material to material. After this discovery the unit of electric resistance has been called the ohm (Ulaby & Ravaioli, 2014).

Four years later, after Ohm's discovery, Joseph Henry discovered that the change in magnetic field create a current on a wire. However, he failed to publish this work. Two years after this work he identified the basic inductor property self-inductance. He avowed the unit of inductance as Henry. After that it was ready to covered by James Clark Maxwell. After these technological developments, it was time to discovery of electromagnetic induction by Michael Faraday in 1831. After discovery of Oersted, which shows the producing of magnetic field with electric current on a wire, Faraday meditate upon why magnetic field cannot produce an electric current. After he noted the discovery of Oersted in 1821, he had worked on this phenomenon. In 1831, Faraday solved the problem and showed that a current can be produced via moving magnet in a copper coil. Also, with this discovery he opened the gates for electric motors.

If we are talking about electromagnetism and electricity, we must talk about the greatest inventor of all of time who is Nicola Tesla. He was the founder of alternating current system. Scientist knew that they cannot send direct current to long distances. At the same time period Nicola Tesla was working on generators. In that time interval he discovered a rotating magnetic field which is the principle of the alternating current. Then he was working on an induction motor and when he built it, it would be the best example for the alternating current. In 1886, Tesla's system was applied to the Niagara Falls for the first time for the first hydroelectric plant in the US. Today we used the unit for magnetic field as Tesla (Ulaby & Ravaioli, 2014).

## 2.2. Magnetic Materials

Magnetic materials show a property magnetic polarization, when exposed to magnetic field. The magnetization can be expressed by linage of the magnetic dipoles of the material when the material within the magnetic field. It is similar to the electric dipoles when the material is inside the electric field. The behavior of the magnetic material is highly nonlinear, and it is only predicted by use of quantum theory. However, most of the engineering applications, it is unnecessary to use. On the other hand, quite good results can be reachable by use of atomic models to show atomic lattice structure of the material.

A magnetic material is expressed by looking at the number of magnetic dipoles. When there is no applied magnetic field, the magnetic dipoles are oriented randomly. Therefore, the vector sum of the magnetic polarization, on a macroscopic scale, is equal to zero (Balanis, 2012).

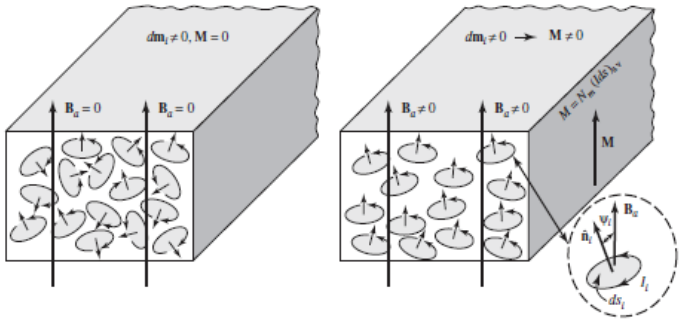


Figure 5. Linage and orientation of magnetic dipoles (Source: Balanis, 2012)

In Figure 5, above, on the left side there is no applied magnetic field, however, on the right side non-zero magnetic field is applied, and magnetic dipoles aligned through the applied magnetic field. In the figure, M is magnetization vector, B is the magnetic flux density, dS is infinitesimal area.

Due to direction of the resultant magnetization vector, materials are ordinated into two groups, which are Group A and Group B.

Group A materials has a property that the net magnetization vector in the material and applied magnetic field has opposite directions, although net magnetization vector is very small in terms of magnitude. Therefore, relative permeability of these materials is slightly smaller than unity. As seen in the table, diamagnetic materials are classified in Group A.

Table 2. Group of materials with respect to magnetic properties (Balanis, 2012)

| Group A | Group B |
|---|---|
| Diamagnetic | Paramagnetic |
| | Ferromagnetic |
| | Antiferromagnetic |
| | Ferrimagnetic |

When we consider Group B materials, the net magnetization vector is added into applied magnetic field. Thus, the relative permeability of these materials is greater than unity. While some of them, such as; paramagnetic and antiferromagnetic, are slightly greater than unity, the others are much greater than unity (Balanis, 2012).

The moments of the electron spins, which occur in diamagnetic materials when there is no magnetic field, oppose to each other, so do the moments of orbiting electrons. Therefore, the resultant magnetic moment in macroscopic scale is zero (Balanis, 2012).

## 2.3. Magnetic Flux and Inductance

- **Magnetic flux:** $\Phi$

$$\Phi(t) = \int_S B(t)dS \tag{2.1}$$

The equation above shows that the magnetic flux is equal to the sum of B-field over a unit area.

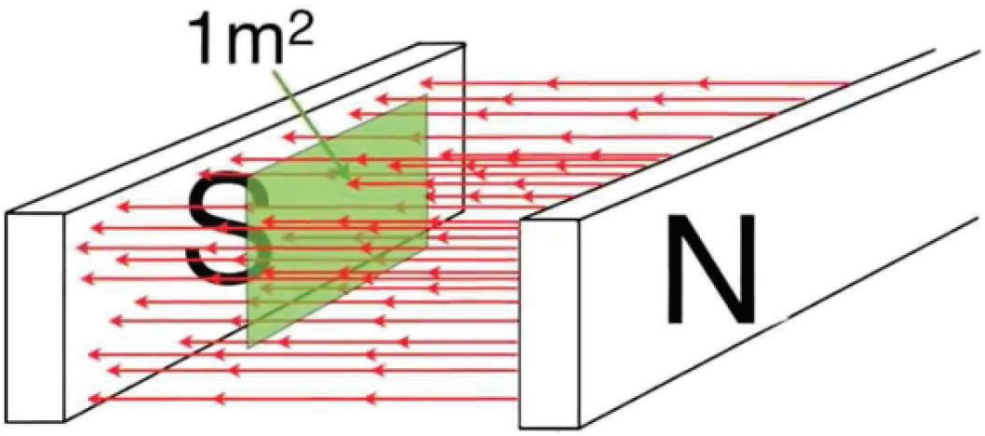


Figure 6. Magnetic flux density (Source: Fizzics Organisation, 2015)

- **Inductance: L**

The relationship between a current and a magnetic field is quite interesting. For instance, while a constant current generates a magnetic field, constant magnetic field cannot generate a current.

On the other hand, magnetic field changing with respect to time generates a current in a loop of wire. For example, suppose that we have 2 loops. When we apply alternating current on one, it generates an oscillating magnetic field on the second loop. Because the magnetic field oscillates, an AC current is observed on the other loop. This magnetic linking is called mutual inductance.

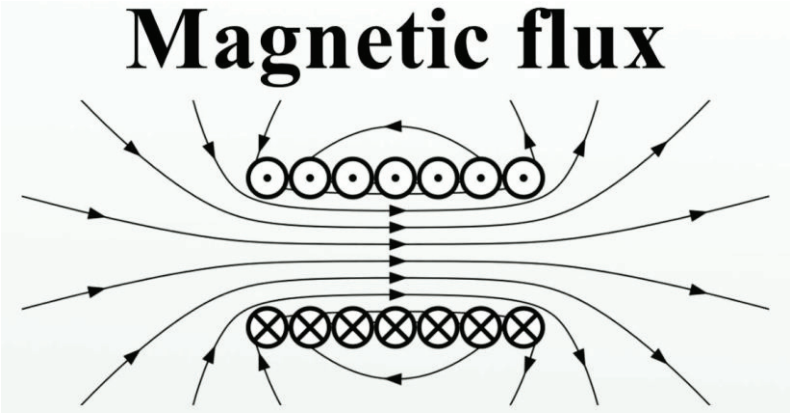


Figure 7. Magnetic Field distribution of a solenoid (Source: Wikipedia, 2019)

We can compute this mutual inductance as shown below:

$$L = \frac{\Phi}{I} \tag{2.2}$$

Where, $\Phi$ is the magnetic flux linkage, I is the current, and L is inductance.

- **Inductance of a solenoid:**

$$H = \frac{NI}{l} \tag{2.3}$$

$$B = \mu \frac{NI}{l} \tag{2.4}$$

For an N loop solenoid, we can write that;

$$L = \frac{\mu \pi r^2 N^2}{l} \tag{2.5}$$

In Eq.2.5, L is inductance of a solenoid, r is the radius of solenoid, $\mu$ is magnetic permeability of the medium of the solenoid, l is the magnetic circuit length, an N is the number of turns of wire.

## 2.4. Maxwell's Equations

Maxwell's equations are one of the most vital conglomerations of formulations of empirical results in history of physics. Maxwell took the experimental laws of Faraday and Ampere and expresses these laws in terms of mathematical way. These equations show the relationship between electric and magnetic phenomenon.

**Equation 1: Gauss' Law**

First Maxwell's equation is the Gauss' Law. This equation indicates the electric field around any charge. This equation can be read as shown below:

$$\nabla \cdot D = \rho_v \tag{2.6}$$

Where, $\nabla \cdot$ is the divergence operation, D is the electric flux density and $\rho_v$ is the electric charge density.

The outcomes of this equation:

- D field lines diverge from any positive charge
- D field lines converge towards any negative charge
- D field lines emanate from or terminate at any electric charge
- The net amount of charge on a surface is exactly equal to the divergence of D field

**Equation 2: Gauss' Magnetism Law**

Where; B is the magnetic flux density. The second law states that the divergence of magnetic flux density is zero.

$$\nabla \cdot B = 0 \tag{2.7}$$

The question is that why divergence of electric flux density has a value rather than zero, but magnetic flux density does not. The answer is quite simple, because there is not a single monopole magnetic charge in the universe. Even one shrinks the volume to an atomic level, magnetic particles have North and South poles. Therefore, the lines never diverge. Also, we can write that;

$$\nabla \cdot H = 0 (because\ B = \mu H) \tag{2.8}$$

**Equation 3: Ampere's Law**

$$\nabla \times H = \frac{\partial D}{\partial t} + J \tag{2.9}$$

Where, H is the magnetic flux intensity, D is the electric flux density, and J is the electric current density. If we write Eq.2.9 in integral form, equation becomes:

$$\oint_C \vec{H} \cdot d\vec{l} = \int_S \vec{J} \cdot d\vec{s} \tag{2.10}$$

In Eq.2.10 $\int_S \vec{J} \cdot d\vec{s}$ is equal to $I_{enclosed}$. We can conclude that if we have a current in enclosed surface, this current will generate a magnetic field around a wire.
We need to note that electric charges create electric field. When the charges start moving, it is called current and only moving charges (current) create a magnetic field. Therefore, we can say that electric and magnetic fields are coupled and travel in space. If we expand these propositions, we will conclude that if there exists an electromagnetic field, there will be an electric field.

**Equation 4: Faraday's Law**

In 1831, Michael Faraday reported several experiments with magnets and motion to cause an EMF on a circuit and to flow current. He induced an EMF in a wire coil, amongst other methods, using:

- Move the coil around or outside of a magnet.
- Stationary holding the coil when shifting the magnet to or away from the coil.
- Stationary keeping the coil close to a fixed electromagnet and adjusting the current via the magnet (and thus the magnetic field that it produces).

The motive EMF, essentially resulting from Lorentz forces on the electrons in moving wires, is an EMF that was caused by the first form. If a magnet is moved or the current is modified via an electromagnet, the magnetic field will be time-dependent and generates a non-potential electric field. This non-potential electric field is the explanation for the EMF that is produced in the stationary loop.

But all Faradays Magnetic Induction methods work in compliance with the same flux law, usually called the Faraday Law of Induction, although their physical roots seem to be different. Whenever the magnetic flow switches through an electronic circuit, and for whatever reason, it causes EMF in the circuit with respect to the formula below

$$\nabla \times E = -\frac{\partial B}{\partial t} \tag{2.11}$$

or,

$$\varepsilon = -\frac{d\phi}{dt} \tag{2.12}$$

While their initial physics is somewhat different from the first, second and third, they have special relativity with each other. In addition, Albert Einstein's work into how methods 1 and 2 produce precisely that same EMF for the same relative motion of the coil and magnet, leading him first and foremost to the special theory of relativity!

Consider moving the long magnet of the thin bar through a coil which is not wider than the magnet as an example of the Law of the Faraday. The flux via the loop increases from the null to the maximum value when the magnet is inserted on the loop, then it remains constant when the loop is shifted by the magnet, and when the magnet leaves the loop, the flux drops back to 0.

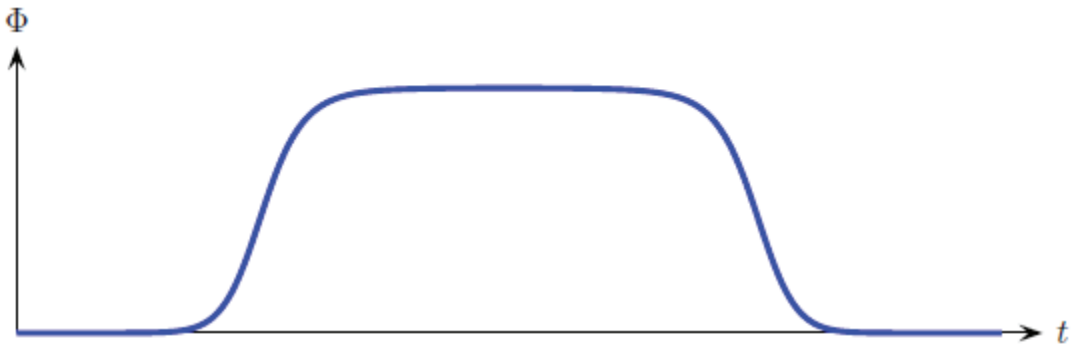


Figure 8. Magnetic flux versus time

In accordance with the Law of Faraday, the flux produces two pulses of EMF, a negative pulse first when a magnet enters the circuit, and then a positive pulse when the magnet goes out and tis can be seen in figure below:

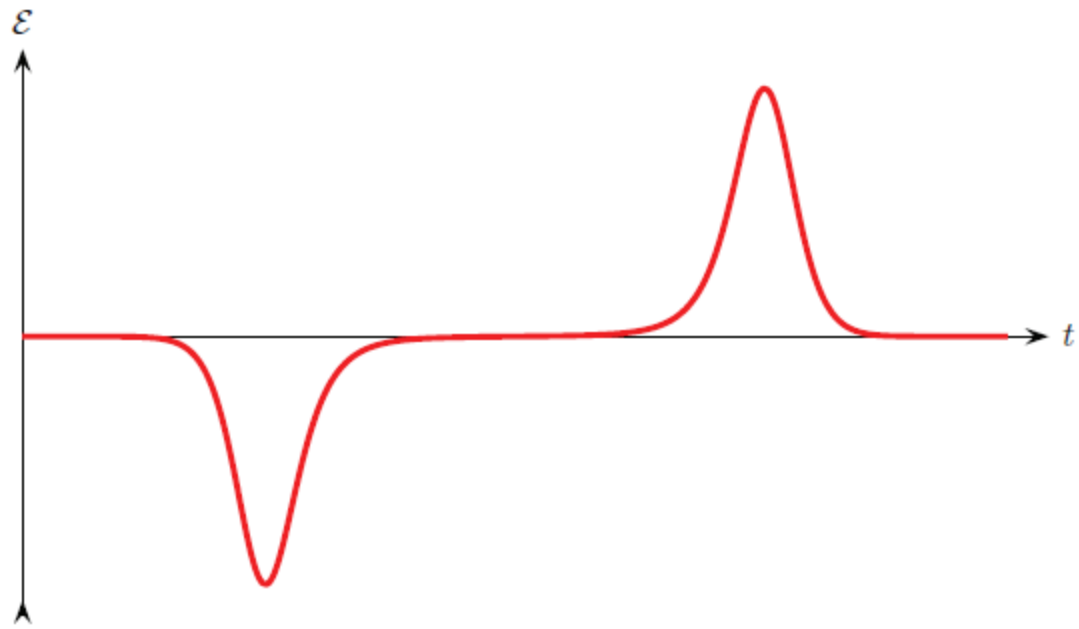


Figure 9. Created EMF signal when magnet enters the coil and leaves the coil

Now we need to look at the direction of the induced EMF due to electromagnetic field. The minus sign in the flux equation encodes the law of Lenz which says the current caused by the EMF attempts to prevent the flux change caused by the EMF. If we speak philosophically; “Nature abhors changing magnetic flux” (Ewing, 1892).

For instance, assume you have a magnetic field upwards through a horizontal wire circuit. Increasing magnetic flow through the loop creates an EMF in the loop in the clockwise direction, resulting in a clockwise current that produces a magnetic field in the

downwards direction. The downward field in the loop attempts to counteract the rising movement of the upward outer field. Also when the external upward field decreased, the declining flux caused an EMF against the clockwise and therefore an upward magnetic field counterclockwise current within the loop which seeks to counteract the decrease in the external upward field (Ewing, 1892).

## 2.5. Sampling Rate

Using analog transducers with digital devices are cost effective and commonplace. Digital data acquisition has many advantages. One of them is efficient handling in terms of control. Another is that large amount of data can be processed rapidly. However, there are basic differences, which gives some limitations and liabilities upon the engineer, between analog and digital systems. The most important difference is that while analog signal is continuous, digital signal is discrete in terms of amplitude and time (Figliola & Beasley, 2010).

The discussion about sampling can be going on with devices which are used in sampling process. Analog signals can be observed with digital devices through analog-to-digital converters. The reverse of previous application with digital-to-analog converters. The other one is between digital and digital devices which interface with an input-output port.

Sampling concept is one of the important things that all the engineers should know. Now, consider an analog signal and its discrete form. If analog signal is processed wrong, some information will be lost (Figliola & Beasley, 2010).

Any continuous dynamic signal can be represented by Fourier series. For reconstructing dynamic signal from a discrete data set, Discrete Fourier Transform (DFT) could be used. The DFT covers all information, which is used to reconstruct the Fourier series of a dynamic signal from its discrete time series. Therefore, Fourier series is one of the best ways to sampling of the continuous dynamic signal.

While digitalizing any continuous analog signal, sampling rate carries very important role. Consider 10 Hz analogue sine wave signal. And sample it successively in every time interval which can be indicated with dt. Then the corresponding sampling frequency $f_s$ will be;

$$f_s = \frac{1}{dt} \tag{2.15}$$

The above discussion can be an example of a constant sampling rate. In every sampling, the amplitude is converted to a number (Figliola & Beasley, 2010).

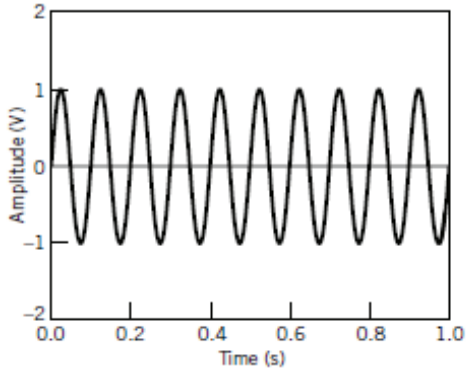


Figure 10. Analog sine wave signal (Source: Figliola & Beasley, 2010)

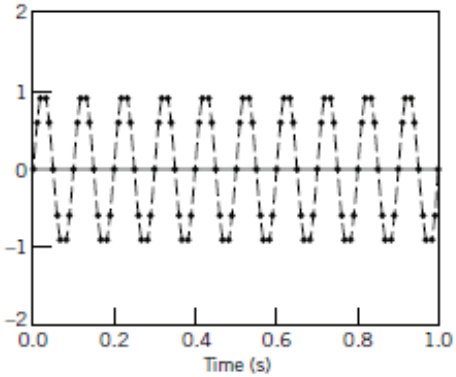


Figure 11. 100 Hz sampling frequency (Source: Figliola & Beasley, 2010)

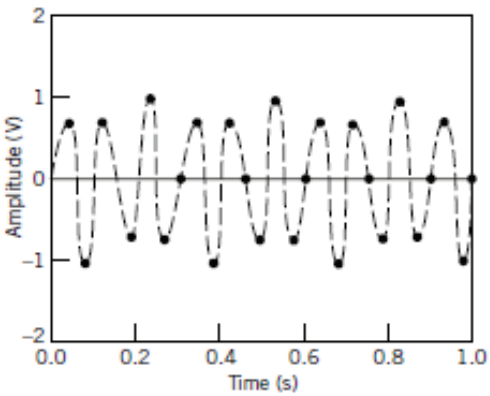


Figure 12. 27 Hz sampling frequency (Source: Figliola & Beasley, 2010)

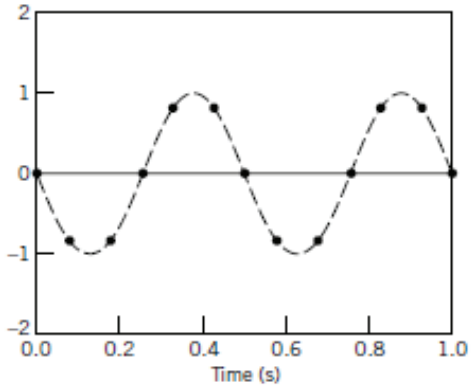


Figure 13. 12 Hz sampling frequency (Source: Figliola & Beasley, 2010)

In Figure 10, above, is represented original analogue signal. There can be easily seen that sampling rate has great role when we digitalized signals. When sampling rate decreases, it is obvious that the amount of information which is carried by analogue signal also decreases. In Figure 12, we can see 27 Hz sampling frequency. In this case, it is obvious that the amplitude information of the signal has been lost. However, in Figure 13, we faced with an interesting phenomenon. We can conclude this phenomenon as; when we decrease the sampling rate, the signal appears at low frequency rather than its true frequency (Figliola & Beasley, 2010).

It is obvious that the sampling frequency has a vital role while representing the frequency of the original signal. The sampling rate theorem states, briefly, that the sampling frequency must be at least two times of the original signal to catch the frequency content of signal. If maximum frequency in the signal showed as $f_m$ and sampling frequency as $f_s$, the sampling theorem shows us;

$$f_s = 2f_m \tag{2.16}$$

or in terms of sample time increment;

$$dt < \frac{1}{2f_m} \tag{2.17}$$

Eq.2.16 and 2.17 indicate required sampling rate and time increment when signal frequency content is important and converting continuous form into discrete form (Figliola & Beasley, 2010).

### 2.5.1. Alias Frequency

Alias phenomenon is one of the important things about information in the signal. Any analog signal is sampled less than $2f_m$ loss its information on the frequency side. The analog signal, which has high frequency content, receives the false ID of a lower frequency in the resulting discrete series. This phenomenon can be seen in Figure 29 in previous subchapter. At the end we misconstrue the frequency of the original analog signal and it gives us wrong information. This wrong frequency is called as alias frequency (Figliola & Beasley, 2010).

Now consider an analog periodic sine signal, with simple function;

$$y(t) = Csin\big(2\pi ft + \beta(t)\big) \tag{2.18}$$

Consider y(t) is sampled with a time increment of dt, this results as;

$$\{y(kdt)\} = Csin\big(2\pi fkdt + \beta(f)\big), \qquad k = 0,1,\dots,N-1 \tag{2.19}$$

If we use the property of $sin\, a = sin(\, a + 2\pi n)$, where n is any integer;

$$\begin{aligned}\{y(kdt)\} &= Csin\big(2\pi fkdt + \beta(f)\big) = Csin\big(2\pi fkdt + 2\pi n + \beta(f)\big) \\ &= Csin\left(2\pi\left(f + \frac{m}{dt}\right)k\delta t + \phi(f)\right)\end{aligned} \tag{2.20}$$

In the above equation m = q, which is an integer number. This results that any frequency of $f$ and $f + \frac{m}{dt}$ can not be distinguished in the sampled series. Hereby, alias frequencies of the signal which has frequency of $f$ can be represented by $f + \frac{m}{dt}$. (Figliola & Beasley, 2010)

To avoid this situation, Nyquist frequency were defined,

$$f_N = \frac{f_s}{2} = \frac{1}{2dt} \tag{2.22}$$

And from Eq.3.22, it can obviously be seen that the sampling frequency must be selected minimum two times greater than the frequency of the systems. In fact, according to experiments, 10 times greater sampling frequency gives the optimal solution.

# CHAPTER 3

# SENSORS AND SYSTEMS

## 3.1. Sensors

In engineering, control of the systems is vital. Especially in the last few decades, systems have gained intelligence and given the condition of the system to users. There are so many types of variables in the system and one of them, for the moving systems, is displacement of some parts or region of the system.

While choosing a sensor for any system, there are some point that the designer must consider. For instance, a company wants to design a robotic arm for the surgery. In the joints, there needs to be angular position sensors. Because of the nature of the surgery, the position and its derivatives are vital. The designer must choose the sensor with high resolution. The output signal delay is important, too. The surgeon must know the position of the end effector precisely. Therefore, the sensor needs to be selected very carefully. In the next sub-chapters, the most important selection criteria are discussed.

## 3.2. Sensors and Systems

A sensor is often described as a tool that is receiving a signal or stimulus and responding to it. This definition is too wide. Actually, it is actually so wide that it covers nearly everything from a human eye to a pistol trigger. For example, let's consider a human in Figure 14,

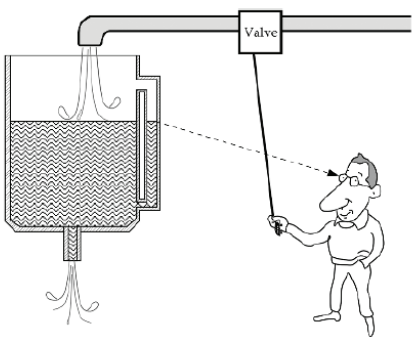


Figure 14. Water level control system

By manipulating its valve, the worker adjusts the amount of liquid in the tank. Changes in the inlet flow rate, temperature fluctuations (this would change the viscosity of the fluid and therefore the flow rate through the valve) and similar disturbances have to be compensated by the operator. The tank is probable to flood or run dry without control. The operator must receive data on the amount of fluid in the tank on a timely basis to behave properly. The sensor perceives the data in this instance, which consists of two main pillars: The sighting tube on the tank and the eye of the worker generating an electrical reaction in the optic nerve. The sight tube alone is not a sensor, nor is the eye a sensor in this specific control system. Only the conjunction of these two parts makes a sensor (detector) that is selectively susceptible to the level of the liquid. If a sight tube is correctly constructed, it will represent fluctuations in the level very rapidly, and it is said that the sensor is respond rapidly. The tube level may delay under the tank level, if the tube's inner diameter is too tiny for a specified fluid viscosity. Then, we should also consider such a sensor's phase characteristic. The delay could be quite adequate in some instances, whereas a better design of the sight tube would be needed in other instances. The efficiency of the sensor must therefore only be evaluated as part of a data acquisition system (Farden, 2003).

This world is split into objects that are made by man and by nature. Natural sensors, like those found in living organisms, generally react with signals, having an electrochemical identity; that is, their physical character is based on transporting ions, as in axons (as in an optic nerve in the worker of the liquid tank). Information is also transferred and processed in electrical form in man-made devices, although through electrons transportation. Sensors used in artificial structures should talk the same language as the interfacing devices. This language is electrical, and a detector made by humans should be able to react with signals where data is transmitted by electrons instead of ions. Then, instead of using an electrochemical solution or a nerve fiber, you can attach the sensor to an electronic system via electrical cables (Farden, 2003).

The aim of a sensor is to react to some kind of physical input property and to transform it into a compatible electrical signal. We might well conclude that a sensor is an electrical translator with a usually non-electrical input. We imply a signal which can be channeled, amplified or altered through electronic appliances when we say ' electrical'. The output signal of the sensor can take the form of current, potential difference or charge. In terms of amplitude, frequency, phase, or digital code, these can be defined further. The output signal format is known as this collection of features. Thus, a sensor has input and

electrical output characteristics. Every sensor is a converter for energy. Whatever you attempt to measure, the energy transfer from the measuring item towards the sensor is always dealt with. The sensing method is a specific case of transferring data and the transmission of data involves power transmission. Of course, the clear fact that energy transmission may occur in both directions. The energy may either flow from an object towards the sensor, or from the sensor towards the object, with a positive sign as well as with a negative sign. For instance, if the object is hotter than the sensor, or when the object is cooler than the sensor, a thermo-pile infrared radiation sensor produces a positive voltage and negative voltage, respectively. The current flow is zero and the output voltage is zero when the sensor and the object are both at equal temperature. As a result, this conveys an indication of the same temperatures (Farden, 2003).

The term sensor must be separated from transducer. The latter is a converter of one sort of energy to the other, while the former transforms all kinds of energy into electrical signal. A transducer is an instance of a loudspeaker which is converting an electrical signal into an acoustic wave and a varying magnetic field. This has no relation to sensing or perception. Transducers can be used in different structures as actuators. An actuator can be defined in reverse direction to a sensor. It usually transforms electrical signal into non-electrical energy. An electrical motor is an actuator, for example. It transforms electricity into mechanical action (Farden, 2003).

There are two kinds of sensors: passive and active. A passive sensor requires no extra power source and produces directly an electrical signal for an external input. Examples include a photodiode, a thermocouple and a piezoelectric sensor. For their operation, the active sensors demand external energy, called an activation signal. The sensor modifies this signal to generate the output signal. The active sensors are sometimes referred to as parametric because their own characteristics change in reaction to an external impact, which can then be transformed to electrical signals. It may be indicated that the parameter of the sensor modulates the activation signal and that the modulation provides measured value data. A thermistor, for instance, is a resistor sensing to temperatures. The electric signal is not generated but its resistance can be measured by identifying changes in present and/or voltage across the thermistor by passing through an electric power (stimulation signal). These ohmic differences connect directly with a known function to temperature. A resistive stress gauge in which the electric resistance is linked to a stress is another instance of an active sensor. Electric current from an external source of energy is required to evaluate the resistance of the sensor.

Sensors can be categorized into absolute and relative according to the chosen reference. An absolute sensor detects a stimulus with regard to an absolute physical scale independent of the measures, whereas a relative sensor generates a signal relating to a specific situation. A pressure sensor is an example of the absolute and relative sensors. A relative pressure sensor generates a signal for a chosen baseline which has nonzero pressure, for example the atmospheric pressure, while an absolute pressure sensor takes the baseline as vacuum.

A sensor can also be viewed with all its characteristics such as measurements, requirements, physical phenomena, conversion system, materials from and field of application. This is another way of looking at a sensor. These properties can be seen below tables (Farden, 2003).

Table 3. Specifications (Farden, 2003)

| | |
|---|---|
| Sensitivity | Stability |
| Accuracy | Speed of response |
| Overload Characteristics | Operating Life |
| Cost, size, weight | Stimulus range |
| Resolution | Selectivity |
| Environmental conditions | Linearity |
| Dead band | Output format |
| Other | |

Table 4. Material of the sensor (Farden, 2003)

| **Inorganic** | **Organic** |
|---|---|
| Conductor | Insulator |
| Semiconductor | Liquid, gas or plasma |
| Biological substance | Other |

Table 5. Detection types which are used in sensor (Farden, 2003)

| |
|---|
| Biological |
| Chemical |
| Electric, magnetic or electromagnetic wave |
| Heat, temperature |
| Mechanical displacement or wave |
| Radioactivity, radiation |
| Other |

Table 6. Conversion phenomena (Farden, 2003)

| Physical | Chemical | Biological |
|---|---|---|
| Thermoelectric | Chemical transformation | Biochemical transformation |
| Photoelectric | Physical transformation | Physical transformation |
| Photomagnetic | Electrochemical process | Effect on test organism |
| Magnetoelectric | Spectroscopy | Spectroscopy |
| Thermoelastic | Other | Other |
| Electroelastic | | |
| Thermomagnetic | | |
| Thermooptic | | |
| Photoelastic | | |

Table 7. Application areas (Farden, 2003)

| | |
|---|---|
| Agriculture | Automotive |
| Civil engineering, construction | Domestic, appliances |
| Energy, power | Environmental, meteorology, security |
| Health, medicine | Information, telecommunication |
| Manufacturing | Marine |
| Military | Recreation, toys |
| Scientific measurements | Space |
| Transportation | Other |

### 3.2.1. Units and Measurements of Sensors

In practice, amount of variable can be either too big or too tiny, it's often not easy to use base or derivative units directly. Multiple and submultiple units are usually used to ease in engineering works. As an illustration, 1 ampere (A) can be multiplied by 10−3 to achieve a smaller unit (mA), which is one milliampere (1 milliampere) or one-thousandth of an ampere (Farden, 2003).

### 3.2.2. Sensor Characteristics

A sensor can have several transformation steps from the input to the output before it generates an electric signal. We consider a sensor to be a "black box" in which only relationships between its output and stimulus signal are considered. However, it is not that simple (Farden, 2003).

### 3.2.2.1. Transfer Function of Sensor

For each sensor there is an ideal or theoretical output-stimulus ratio. The performance of such a sensor would always be the real value of the stimulus if it is properly designed and manufactured with excellent materials by excellent employees using excellent instruments. The ideal function can be described as a value table, a graph, or a mathematical equation. The so-called transfer function characterizes an ideal (theoretical) connection between output and stimulus. This feature determines the reliance between the sensor-generated electric signal U and stimulus u (Farden, 2003). In a very basic form;

$$U = a + bu \tag{2.1}$$

where "a" (i.e. the signal output at the zero-input signal) is intercept and the "b" is the slope is called sensitivity sometimes. U is one of the features of the electrical output signal which is used as the sensor output by data acquisition systems. Depending on the sensor characteristics, it may be amplitude, frequency, or phase. The sensor does not have to have linear relationship between stimulus and output. It may have logarithmic, exponential or power function (Farden, 2003).

### 3.2.2.2. Full Scale Input (Span)

An input full scale (FS) is called a dynamic range of stimuli that can be converted from a sensor. This is the largest possible stimulus to the sensor without causing an unacceptable inaccuracy.

### 3.2.2.3. Full Scale Output

The algebraic difference between the electric outputs with a maximum input stimulus and the lowest input stimulus is defined as a Full-Scale Output (FSO).

### 3.2.2.4. Accuracy of Sensor

A significant feature of the sensor is accuracy, which implies genuinely inaccuracy. Inaccuracy is defined as the largest deviation from the sensor's optimal or true input value. The distinction between the value calculated from the output voltage and the real value of the input can be defined as a deviation (Farden, 2003). A linear displacement sensor, for instance, should ideally produce about 1 mV per 1 mm drive, that is, the transfer function of the sensor is linear and has a slope, which means sensitivity, of *slope=1mm/mV*. In the experiment, however, an output of U=10.5 mV was generated with a displacement of u=10 mm. The additional 0.5 mm can be defined as an erroneous measurement or error deviation. In a range of 10 mm the complete inaccuracy of the sensor is therefore 0,5 mm, or in relative terms (0,5mm/10 mm) the inaccuracy is 5 percent. Repeating this experiment again and again with no random mistakes and every time we see a 0,5 millimeters mistake, we can say that the sensor has a 0,5 millimeters systemic inaccuracy over 10 millimeters. Of course, there is always an random constituent so that the systematic mistake can be shown as an average or average multitasking value. There are several ways to show the inaccuracy rating. For example:

- Regarding the measured value directly (which means delta)
- The percentage of full-scale input (span)
- Regarding the output signal

For instance, resistive displacement sensor has 100 mm full scale input and 10 ohms full scale output. Inaccuracy of this sensor can be defined as +/- 0.5%, +/- 0.5 mm, or +/- 0.05 ohms.

### 3.2.2.5. Calibration of Sensor

The calibration of the sensor has really vital role in measurement. For example, we need to measure the displacement with an accuracy of 0.1 mm, but our sensor has (physically) 0.2 mm accuracy. Does that mean that we cannot use this sensor? Of course not. The sensor needs a calibration. It means that we need individual transfer function for that particular sensor (Farden, 2003). Calibration implies determining particular variables describing the total function of transfer. Total implies for the whole system, including

sensor, circuit interface and A/D converter. Before calibration, you should know the mathematical model of the transfer function.

In order to calibrate sensors, precise physical norms of the suitable stimuli need to be correctly maintained and preserved. For instance, a blackbody cavity would be required to calibrate the infrared sensors or a number of saturated salt solutions are needed for calibration of an hygrometer in a closed container to maintain a permanent relative humidity, and so on (Farden, 2003).

### 3.2.2.6. Hysteresis

A hysteresis error is a distortion of the output of the sensor at the designated stage of the input signal when approached from the reverse direction. For example, when the object moves from left to right at a certain point, a displacement sensor generates a Voltage that differs by 20 mV from that of the object moving from right to left. The error in hysteresis with regard to movement units is 2 mm if the sensitivity of the sensor is 10 mV/mm. Friction and structural modifications in the fabrics are typical triggers for hysteresis (Farden, 2003).

### 3.2.2.7. Saturation of Sensor

There are working boundaries for each sensor. Although deemed linear, its output signal is no longer responsive to some concentrations of the input stimuli. An additional increase in stimulation does not generate a desirable output. The sensor is said to have a span-end nonlinearity or saturation. It can be seen in Figure 15.

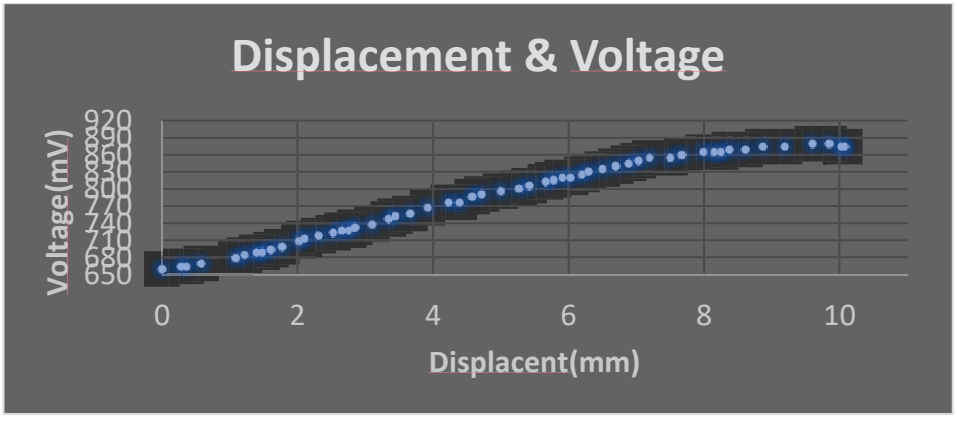


Figure 15. Transfer function with saturation of the sensor after 8 millimeters

It is obviously seen that after 8mm the sensor leaves the linear span region and starts entering saturation region (Tanriyapisi & Ozdemir, 2017).

#### 3.2.2.8. Resolution

Resolution defines the least sensitive increments of stimulation. If a stimulus differs continually across the spectrum, even under noise circumstances, the output measurements of some sensors will not be smooth. Every signal transformed into a digital format is also broken down into tiny measures in which each step is allocated a number. In given circumstances, the magnitude of the input variability that results in the lowest output phase is defined as resolution. For example, 0.5-degree resolution may be specified as 0.181% of FS (Full Scale) for an angular sensor with 270 degrees full scale (Farden, 2003).

The digital output sensor resolution is determined by the number of bits in the data word. The resolution may, for example, be specified as 8-bit resolution. In order to make sense, either the value FS or LSB (least significant bit) is required for this declaration. When the output signal does not have measurable steps, the sensor says its resolution is infinitesimal or continuous. However, sometimes this specification mistakenly known as infinite resolution (Farden, 2003).

## 3.3. LVDT (Linear Variable Displacement Transformer) and Usage Areas

Although variable differential transformers were invented earlier, linearly variable differential transformers were introduced as a position sensor in 1940 by G. B. Hoadley. At first it was used mostly in military applications, because sensor is robust and rugged, and quality applications, because of having high resolution. Essential improvements in construction and performance were made up to 1960s. Then LVDT was started using in industrial applications.

LVDT (Linear Variable Displacement Transformer) is an electromechanical displacement transducer in which working principle is an induction. LVDT has many advantages when the other displacement transducers are considered. First of all, it is frictionless. Therefore, mechanical life of core is infinite. Secondly, it provides infinite

resolution. In here, infinite means that the resolution of the remaining peripherals in circuitry. As it is known, the magnetic field is not the same, when the core moved in attometer ($10^{-18}$) scale. Furthermore, LVDT has single axis sensitivity, so that is the situation in the proposed issue. Also, repeatability of the sensor is high, because of its robustness. It is not effected from dust and dirt (Blejan et al., 2016).

There are mainly two disadvantages about LVDT. The exciting frequency affect the output signal because output signal is a function of phase difference. Therefore, it needs to be constant and certain. According to phase dependence of LVDT cabling is a problem that needs to be overcome (Blejan et al., 2016). The other problem is LVDT needs relatively complex electronics when it compared to other types of displacement transducers (Drumea et al., 2006).

Although, LVDT is not suitable for the present issue, the working principle is very similar with Accuciser. They both work with electromagnetic principle. Therefore, in Chapter 4, the experiment set starts with an LVDT to decide the number of windings for primary and secondary coils and the diameter of the copper wire. These results can be used in Accuciser too.

# CHAPTER 4

# EXPERIMENTS AND RESULTS

## 4.1. The Effect of Number of Windings and Diameter of Copper Wire on Output Signal of LVDT

One of the most important parameters that affect the LVDT is the winding properties of LVDT. To optimize the winding parameter there had been made 10 different experiment by the author. In the light of these experiments the optimal solution was investigated.

For the signal conditioning of the LVDT PIC16F877A microcontroller were used in all experiments. The output signal of LVDT is AC signal. Therefore, the reading algorithm in the microcontroller was iterative and response time is late when it is compared to commercial LVDT signal conditioner. However, in these experiment sets the aim was only to investigate the effect of winding properties. Thus, the effect of late response does not change the results. The block diagram of the experiment can be seen in Figure 16.

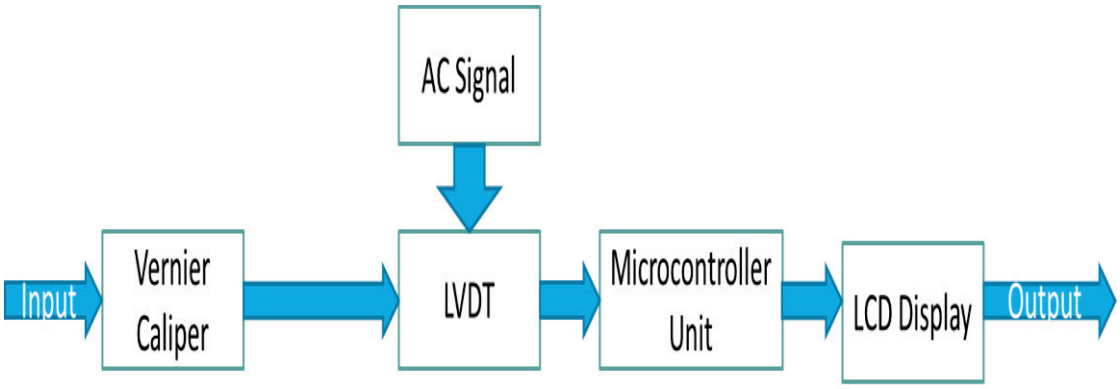


Figure 16. The block diagram of the experiment set

In the following table, the parameters, that are remains constant all of the experiments, is shown in Table 8;

Table 8. Constant variables of the experiments

| | |
|---|---|
| The outer diameter of the inner shell | 3.40mm |
| The material of the inner Shell | Silicone |
| The outer diameter of the core | 2.50mm |
| The material of the core | Pure iron |
| The material of winding wired | Copper |
| The input signal frequency of the primary winding | 17kHz |
| Primary winding voltage | $4V_{p-p}$ |
| Resolution of the Vernier caliper | 0.01mm |
| Full stroke measurement | 10.00mm |

In all set-ups, Vernier caliper and sensor prototypes were fixed onto ground, and the core was moved with depth measuring blade of Vernier caliper. The specifications of the experiment sets are indicated in Table 9 below.

Table 9. Specifications of the experiments

| Experiment No. | Number of primary winding | Number of secondary winding | Primary winding wire diameter(mm) | Secondary winding wire diameter(mm) | Maximum drawn current(mA) |
|---|---|---|---|---|---|
| 1 | 10 | 10 | 1,00 | 1,00 | 110 |
| 2 | 10 | 20 | 1,00 | 1,00 | 110 |
| 3 | 20 | 10 | 1,00 | 1,00 | 110 |
| 4 | 25 | 25 | 0,50 | 0,50 | 140 |
| 5 | 25 | 50 | 0,50 | 0,50 | 140 |
| 6 | 50 | 25 | 0,50 | 0,50 | 130 |
| 7 | 25 | 50 | 0,50 | 0,12 | 130 |
| 8 | 50 | 25 | 0,12 | 0,50 | 120 |
| 9 | 50 | 50 | 0,12 | 0,12 | 120 |
| 10 | 50 | 100 | 0,12 | 0,12 | 110 |

As can be seen in the table, when the magnetic circuit length increases, current is drawn in primary winding increases. However, because of some uncertainties in Exp.6, although the magnetic circuit length is greater than the Exp.5, the drawn current is less than it. One of the uncertainties in the experiment is that the sensors were not manufactured with automation but handmade. Therefore, windings wire in Exp.5 and Exp.6 may have some cross-sectional differences in sub-millimeter scale.

- **Experiment No.1:**

In Exp.1 number of primary and secondary winding are equal and 1.00mm diameter wire was used. As can be seen clearly from the Figure resolution of the device is 2.66mm. For analog displacement sensors this type of resolution cannot be acceptable. Furthermore, the range of the device is not 10.00mm. Because after 7.98mm the voltage remains constant and did not increase with the displacement of the core.

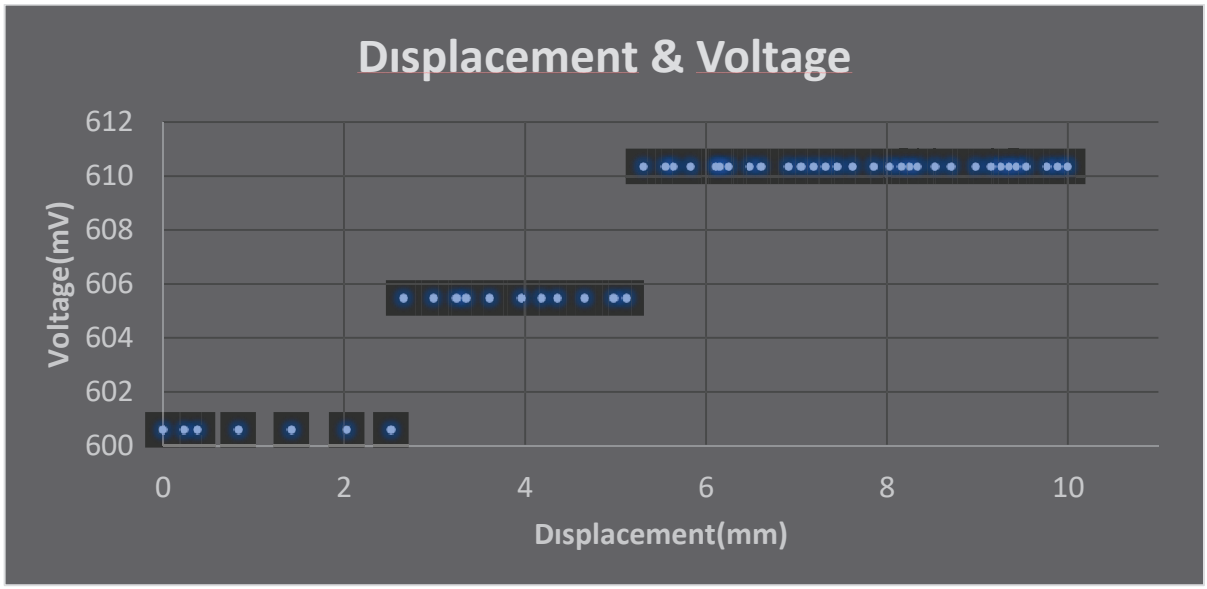


Figure 17. Displacement-Voltage curve of Exp.1

- **Experiment No.2:**

In this set-up sensor has 10 and 20 windings primary and secondary relatively. As shown in the figure voltage does not change along the full stroke displacement. Primary coil generates time dependent magnetic field, but displacement of core does not change

the flux density along secondary winding. Correspondingly, there was observed no voltage changing output signal of secondary winding.

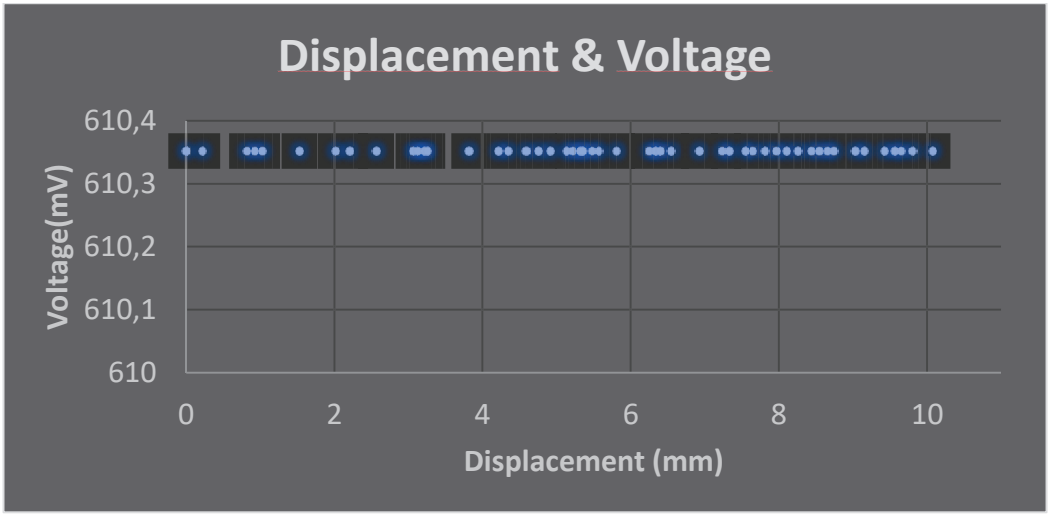


Figure 18. Displacement-Voltage curve of Exp.2

- **Experiment No.3:**

The windings were changed in this experiment with respect to Exp.2. Again, along the full stroke displacement, output voltage of secondary winding remains constant. However, if Exp.2 and Exp.3 are compared, the voltage induced in the secondary windings are different. By the definition, inductance of a coil is directly proportion with number of windings. By extension, it can be said the more inductance the more voltage.

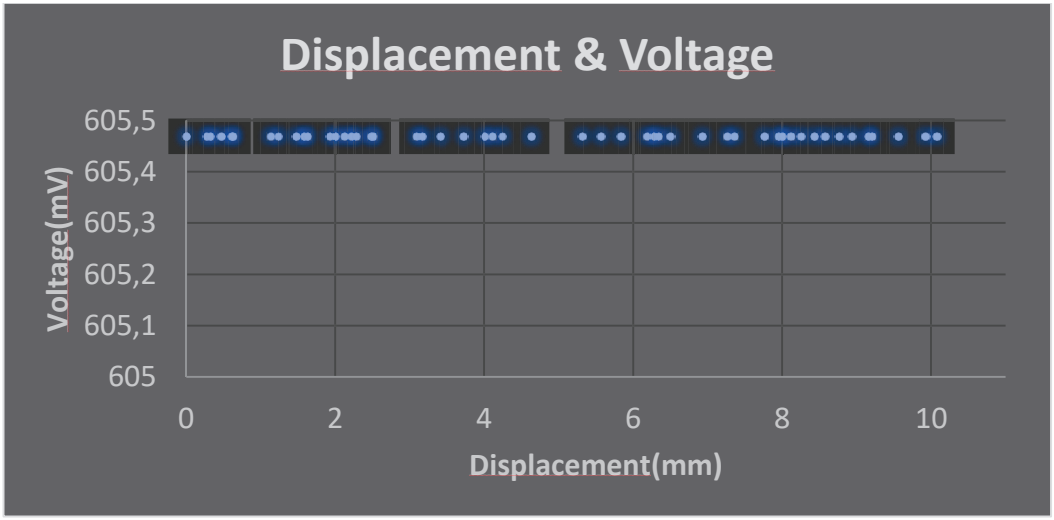


Figure 19. Displacement-Voltage curve of Exp.3

In the light of these three experiments we can say that choosing large diameter wire for windings is not wise selection. In addition to this, choosing primary windings less than secondary winding would be a better choice.

- **Experiment No.4:**

In the light of first three experiment, for the next step, we decided to reduce wire diameter to 0.50mm. The number of windings is equal both in primary and secondary and a value of 25 wounds. Figure shows that, the resolution is a bit higher than the first experiment. However, the voltage changing along the full-scale displacement is not constant. For example, in between 0 and 2.63mm the voltage difference is 4.88mV. However, in between 2.63mm and 4.85mm the voltage difference in secondary winding is 4.88mV. It can be clearly concluded that in the first change occurs with shifting the core 2.63mm, but in the second change occurs with 2.22mm shifting of the core. Because of changing resolution, this is also not a wise choice to select winding parameters as in this experiment.

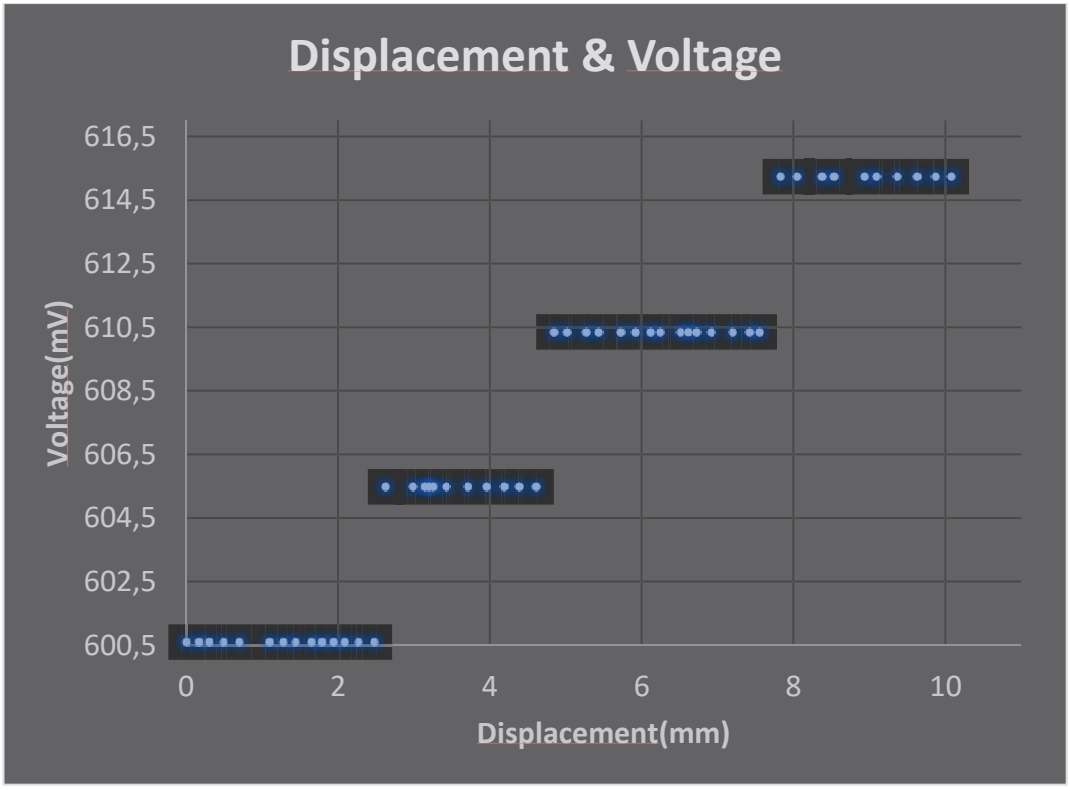


Figure 20. Displacement-Voltage curve of Exp.4

- **Experiment No.5:**

The induced voltage is greater because of secondary winding has more wounds. However, as same as the Exp.4, resolution is changing in full stroke measurement. The figure shows also step sizes are getting smaller. This trend shows us that we are getting similar to ideal LVDT curve.

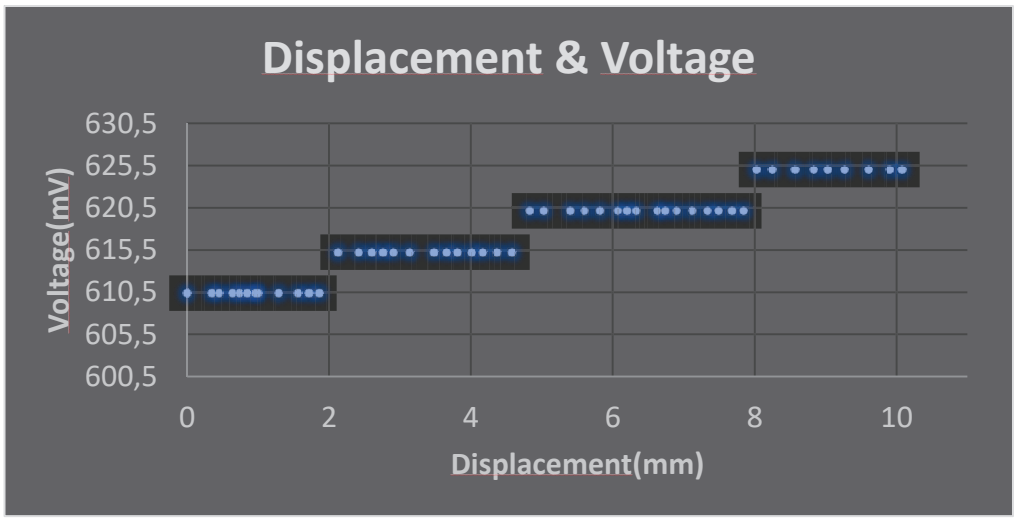


Figure 21. Displacement-Voltage curve of Exp.5

- **Experiment No.6:**

In Exp.6 primary winding is doubled with respect to secondary coil. This device gives the results as same as Exp.3. Therefore, again, designing primary winding larger than secondary winding is not a wise choice. Because the results are not acceptable.

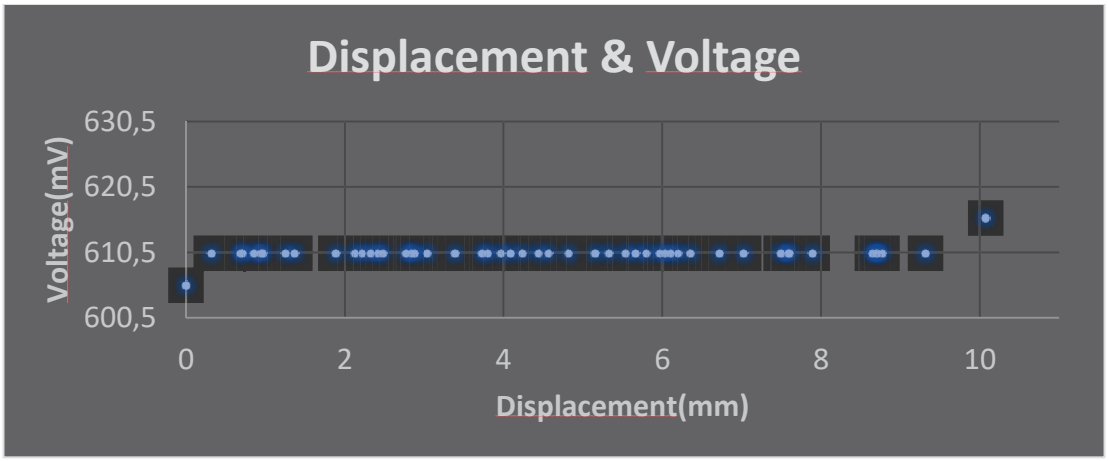


Figure 22. Displacement-Voltage curve of Exp.6

- **Experiment No.7:**

The results are contradictory in Exp.7. In this device, two different diameters are used for the wires. While primary winding has 25 turns and a diameter of 0.50mm wire, secondary winding has 50 turns and a diameter of 0.12mm wire. It can be easily seen that the results are not changing with an any trend. Therefore, it is not preferable while designing an LVDT.

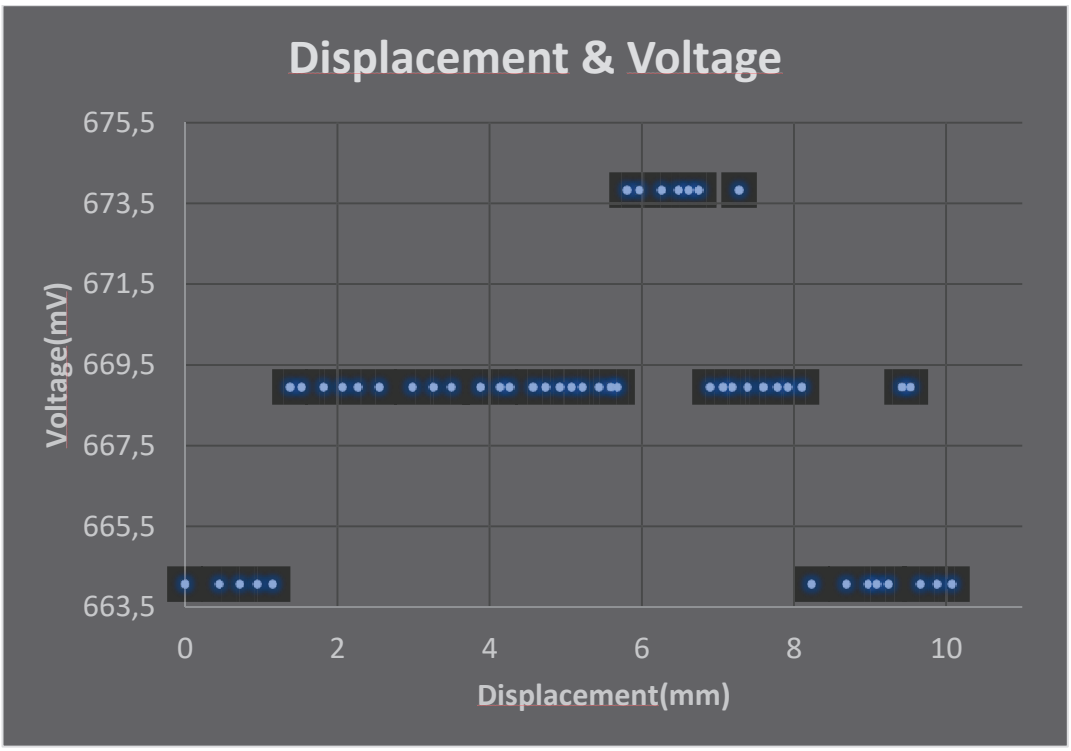


Figure 23. Displacement-Voltage curve of Exp.7

- **Experiment No.8:**

In this set-up, the trend of the results getting closer to the linear LVDT. We can identify that because after 6.13mm voltage level has decreasing behavior. In ideal LVDT, up to some displacement behaves linearly increasing. However, after that point the device lose its linearity and becomes decreasing nonlinearly. Again, the resolution of the device is not constant and poor in this set-up. Therefore, it would not be a wise choice to select these parameters to manufacture LVDT.

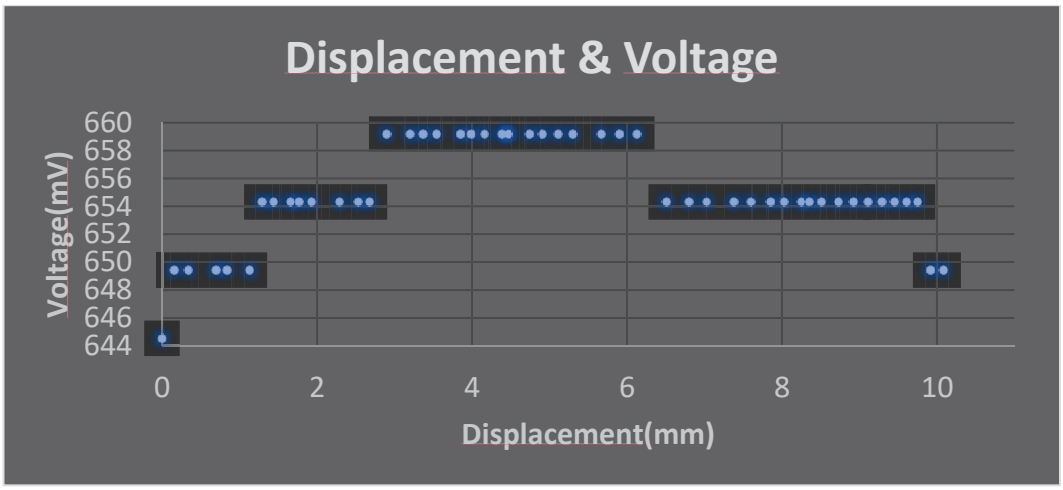


Figure 24. Displacement-Voltage curve of Exp.8

- **Experiment No.9:**

After first eight experiment, we decided to decrease the outer diameter of the copper wire. As shown on the Table, number of primary and secondary winding was chosen to be 50 wounds. Figure indicates that we become getting closer to ideal LVDT. However, there are some wrong data appears in the figure. Normally the data has to be increase while displacement of the core increases. However, with the results that we get from Exp.9, we can say that we are on the right way.

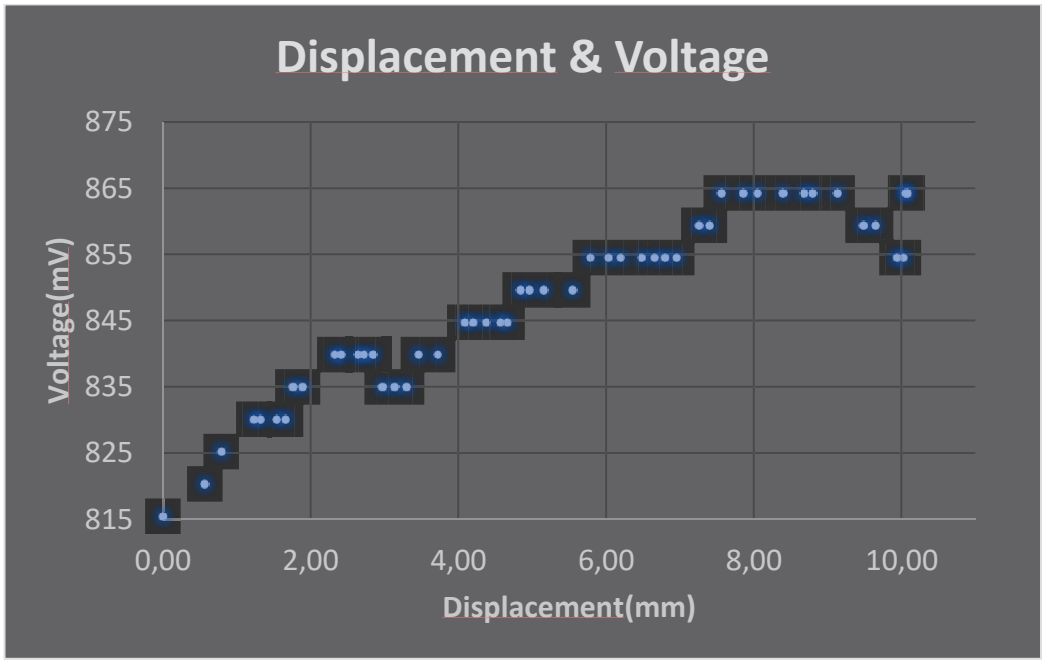


Figure 25. Displacement-Voltage curve of Exp.9

- **Experiment No.10:**

In this prototype, the results are satisfying when they are compared with the first nine experiments. We can easily see that when the displacement increases, the voltage coming from the secondary winding also increases up to 9.19mm. After this point, device enters the nonlinear region. The range of voltage is huge when it is compared with other nine experiments. It is a good result because of visibility of changing and readability of resolution of device.

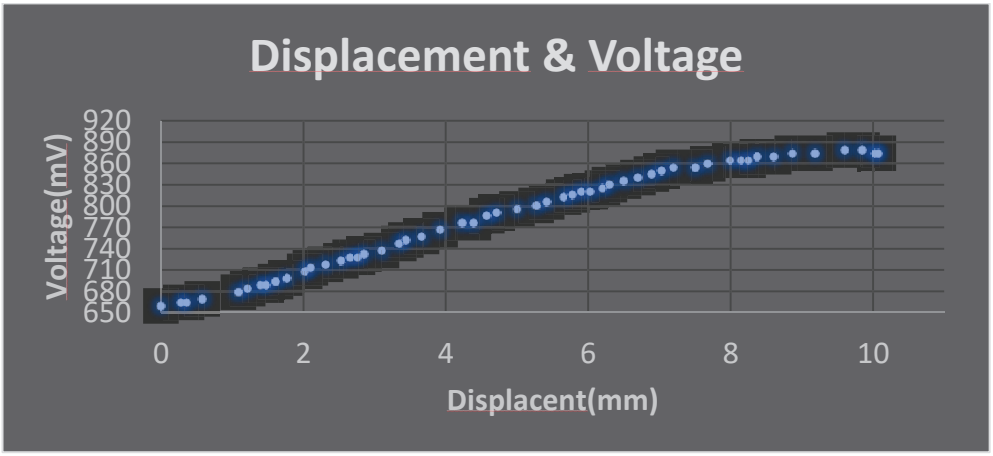


Figure 26. Displacement-Voltage curve of Exp.10

After this work, we can say that number of windings and diameter of copper wire have non-negligible effects on the resolution of LVDT. When small diameter of copper wire was used, the power consumption reduces. High resolution can be reachable with small diameter copper wire. Also, we investigated that choosing number of primary winding less or equal then the secondary winding would be wiser according to the performed experiments. The noise in the output signal is much larger when large diameter of copper was used. As a result, to produce a high resolution LVDT, the optimized parameters are given below;

- Number of primary winding: k
- Number of secondary winding: 2k
- Diameter of copper wire of primary winding: D
- Diameter of copper wire of secondary winding: D
- Diameter of copper wire of both primary and secondary winding: Less than 0.50mm.

## 4.2. Application of Magnetism Formulas to Present Study

In our situation, the solenoid is wound on a ferromagnetic material. When we apply a current in a solenoid, the material steals the magnetic field lines. Therefore, we need to saturate the wall thickness of the material with a magnetic field lines. Then the material will act like an air in terms of magnetic properties.

We need to find the saturation current for present situation. For this, the inductance formula shall be written as follows,

$$\Phi = BS_{wallthickness} \tag{3.13}$$

$$I = \frac{\Phi l}{\mu SN} \tag{3.14}$$

The saturation values are changing with respect to materials. These changing is illustrated in Figure 27:

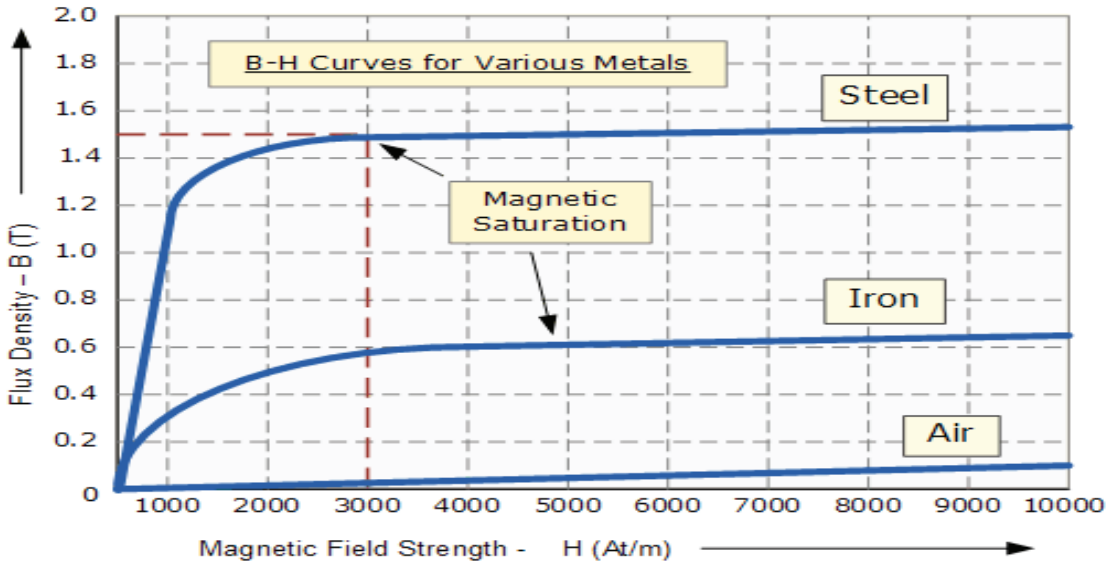


Figure 27. B-H curve for different materials (Source: Rathor, 2017)

In the injector, there were made some calculations and assumptions and they are listed on the next page.

- Relative magnetic permeability of injector: 100
- The solenoid is perfect and ideal
- Calculation of critical current in Table 10

In Table 10, radius of wire of solenoid is changing. Therefore, with a constant magnetic circuit length, number of windings change. We can easily see that when the number of coils increases the required current (critical current to saturate the injector) decreases. However, manufacturing of coils which have tiny wires a bit hard. On the other hand, if we do the coil with two or more layers, we can overcome this problem. In the next heading this solution will be investigated.

Table 10. Minimum current requirements for saturation of wall thickness of injector

| $r_{wire}$ (m) | $r_{outer}$ (m) | $r_{inner}$ (m) | B (Tesla) | H(A/m) | $S_{wall}$ ($m^2$) | L (m) | μ (magnetic permeability) | N (number of turns) | Required current (A) |
|---|---|---|---|---|---|---|---|---|---|
| 0,000025 | 0,004000 | 0,0016 | 1,600 | 12000 | 4,2223E-05 | 0,003 | 0,000133333 | 60 | 0,504 |
| 0,000050 | 0,004000 | 0,0016 | 1,600 | 12000 | 4,2223E-05 | 0,003 | 0,000133333 | 30 | 1,008 |
| 0,000075 | 0,004000 | 0,0016 | 1,600 | 12000 | 4,2223E-05 | 0,003 | 0,000133333 | 20 | 1,512 |
| 0,000100 | 0,004000 | 0,0016 | 1,600 | 12000 | 4,2223E-05 | 0,003 | 0,000133333 | 15 | 2,016 |
| 0,000125 | 0,004000 | 0,0016 | 1,600 | 12000 | 4,2223E-05 | 0,003 | 0,000133333 | 12 | 2,52 |
| 0,000150 | 0,004000 | 0,0016 | 1,600 | 12000 | 4,2223E-05 | 0,003 | 0,000133333 | 10 | 3,024 |

In Figure 28 below, until the saturation point, material of injector nozzle steals the magnetic flux and does not allow to flux to reach to the needle.

After saturation, which means that we apply the minimum required current to the solenoid shown in Figure 29, the magnetic flux effuses from the wall thickness and it reach to the center of injector theoretically. This leakage is caught by the injector needle. The moving injector needle generates time varying magnetic field. Therefore, this time varying magnetic field will generate an electromotive force on the secondary winding. The potential difference, due to electromotive force, indicates the changing displacement of the moving injector needle. Both in Figure 28 and Figure 29 red lines illustrate the magnetic flux.

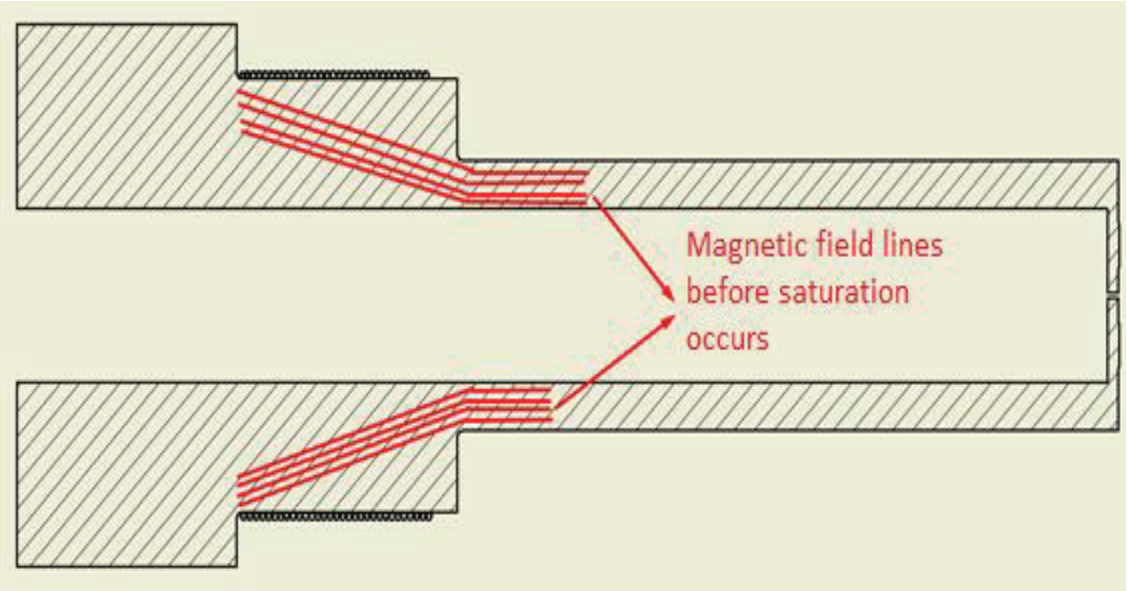


Figure 28. Saturation of wall thickness of injector

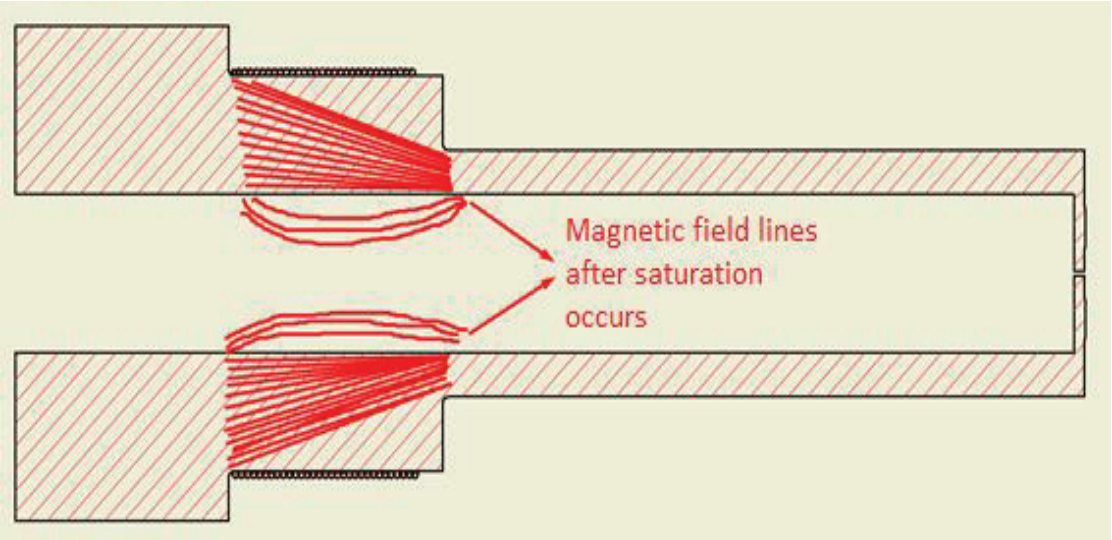


Figure 29. Saturated injector

## 4.3. Novel Inductive Displacement Sensor

In the automotive industry, internal combustion engine technology is at its borders. Therefore, minute improvements make huge differences in terms of efficiency and popularity. To this end, sensors would obviously be of great help to give many helps to developers.

We know how combustion occurs in the Otto cycle in theory. In spite of the fact that automotive technology has advanced in parallel to the digital age and the progress in AI (Artificial Intelligence), it is surprising that there is no clear-cut solution to the problem of combustion timing in a cylinder. As one already knows that combustion timing is the key to engine power, torque, emissions etc. What is meant by combustion timing is the start and the end of the combustion inside the cylinder. There is research to monitor the combustion inside a cylinder in real time. Even though a series of researchers could manage to monitor inside of a cylinder during the operation of an internal combustion engine, but none of these researches was devised for real life, and instead they are all meant for research with very limited monitoring capability for a very limited time duration. It is known that many researchers have been working about this topic. However, these studies have mostly lingered in academic world.

Our new sensor works with inductive principle. As mentioned in previous Chapter, LVDT is one of the most powerful displacement sensors in terms of robustness and high resolution. Although it is powerful, it has some weaknesses and disadvantages. One of them is LVDT operates on alternating current. Therefore, it needs to have signal generator to work. Another disadvantage is that, again, AC signal. As we know if you work with magnetic field which is changing by time, you will need to have paramagnetic material for housing of the core. The reason is that there is a limitation for the skin that magnetic flux penetrates. This phenomenon is known as skin effect.

In the skin effect, the depth, that magnetic flux penetrates, and the frequency of the current, that generates the magnetic field in a solenoid, and magnetic permeability of the housing are inversely proportional. To sum up, if the housing is metal, using alternating current to generate a varying magnetic field will not be a wise choice.

In the proposed system, the housing of the core is metal, which is a valve guide. Therefore, lower frequencies are needed to observe changes in the potential difference in secondary winding. However, this scheme imposes its own limitations as well. If one keeps the magnetic field generating frequency low, no observable current on the secondary winding will be induced. By virtue of Faraday's law, the reader may recall the natural corollary that the higher the frequency the higher the induced voltage at the output.

Aforementioned disadvantages and challenging physical limitations have led to a new inductive displacement sensor. At the starting of the next page the comparison of the Accuciser and conventional LVDT can be seen;

- Accuciser works with DC current.
- Accuciser has two windings, not three.
- The windings are not wounded side by side, they are wounded one on the top of the other.
- It does work, when the housing is metal.

If we mention about disadvantages;

- It needs high voltage and current.
- The output signal is too noisy.
- The core must be in motion, as the core generates varying magnetic field to generate a current on the secondary winding. Otherwise, no voltage output would be observed.

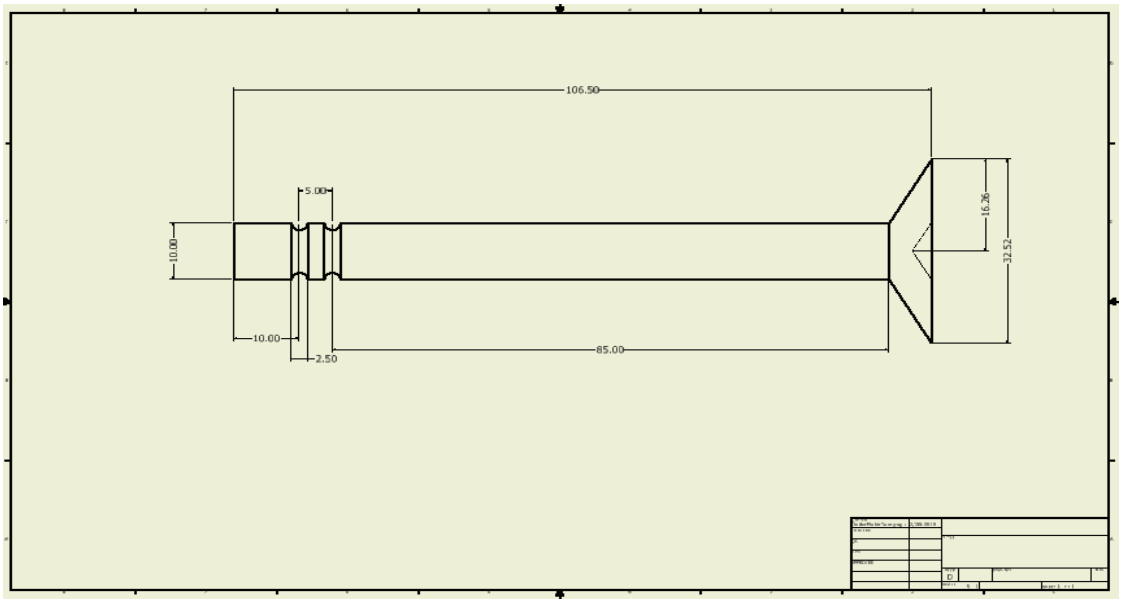


Figure 30. Technical drawing of the valve

In current experiment, valve guide is made of bronze. The relative permeability of bronze is nearly 1. However, because of being metal it does not allow to magnetic flux to pass wall thickness and reach the core. Therefore, LVDT has no use in this situation. Accuciser is suitable in this situation. The properties of the first prototype are given below:

- The primary and secondary windings are wounded side by side.
- Number of winding of primary: 25
- Number of winding of secondary: 50
- Voltage: 25 V
- Current: 2.2 A

As you can see in the Figure 31 and Figure 32 below, when the core moves, because of notches on the valve, displacement can be observed from the data. There are two peaks in the data and the meaning of these peaks are given below:

- When the first notch passes the secondary winding, the magnetic flux that are leaving the valve from the notch, starts generating current on the secondary winding. When the second notch has effect on secondary winding, the second peak starts being generated.
- The amplitude of the second peak is less than that of the first peak. The reason is that when the valve preparing to go back it needs to slow down. Because of slowing down of valve generated voltage is smaller. This comes from Faraday's experiment.

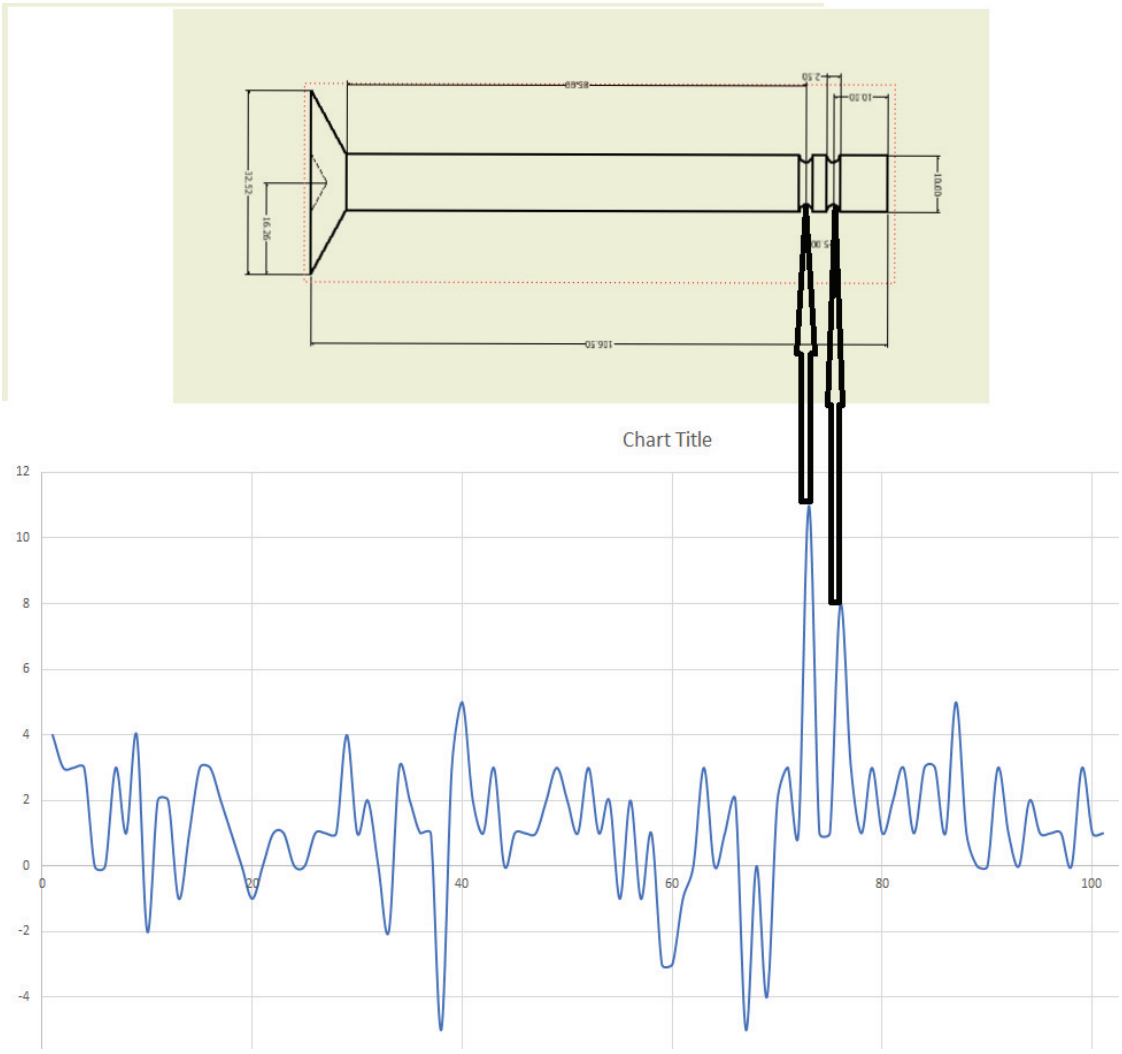


Figure 31. Proof of effect of the signal with respect to notches on the valve

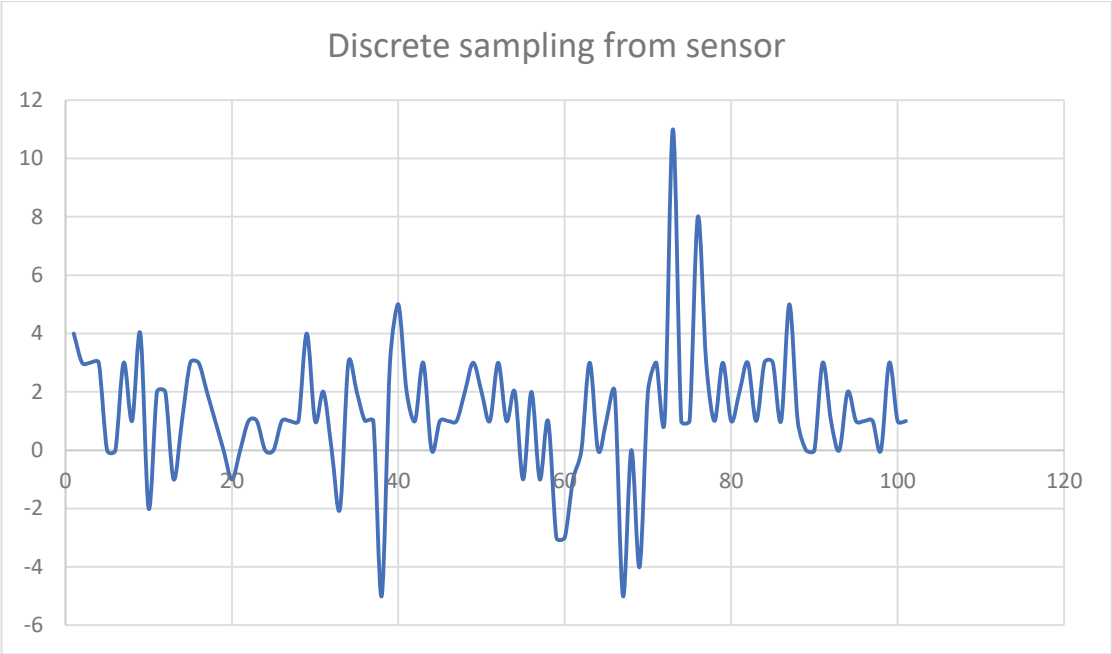


Figure 32. Engine valve displacement

### 4.3.1. System Model and Output of Sensor

At this time, the sensor is integrated with the moving system whose actuator is electromagnetically actuated linear valve. The system model is illustrated in Figure 33.


Figure 33. System model of the experimental setup

In this experimental setup, instead of valve, pure iron core is used as a valve. There is a notch on the core to simulate valve cross-section and the section, where the sensor is mounted, is thinned out. Although the material is bronze it has a relative magnetic permeability of 1.20, saturating the thickness with magnetic flux is hard to achieve. This thinning out has also advantage that when you use thin skin that magnetic field overcome, the sensor needs less current and voltage. Therefore, power consumption, which is highly important in automotive, aeronautical industry etc., become less. Figure 34 and Figure 35 show the valve guide with the sensor and the valve which has notch on it.

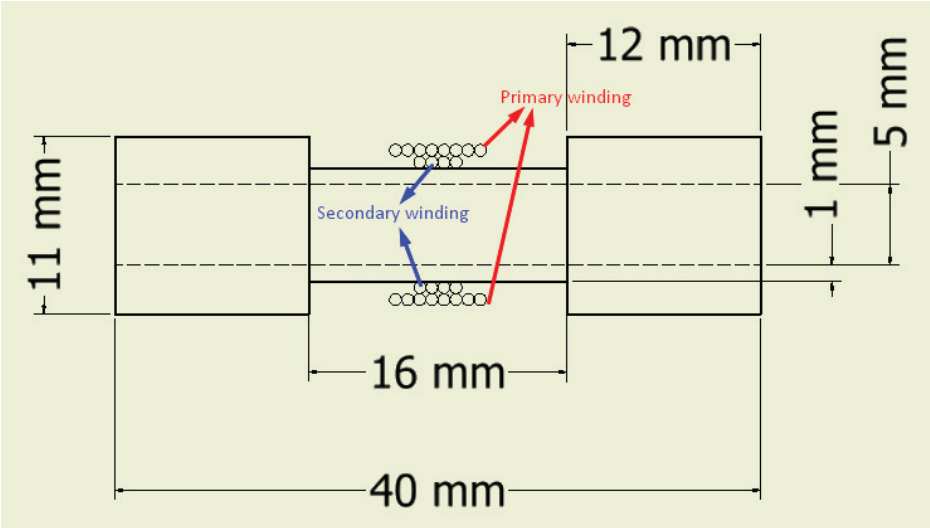


Figure 34. Illustration of the valve guide and the sensor

The sensor is located on the trimmed section of the valve guide as shown in Figure 34. The alignment of the sensor is that the secondary winding is located on the valve guide, and on the top of secondary winding, primary winding is located. In the previous prototype, the windings are located next to each other. This causes a noise in the signal. The reason is that the magnetic field cannot dominate completely the secondary winding. Therefore, the output signal becomes weak against noise.

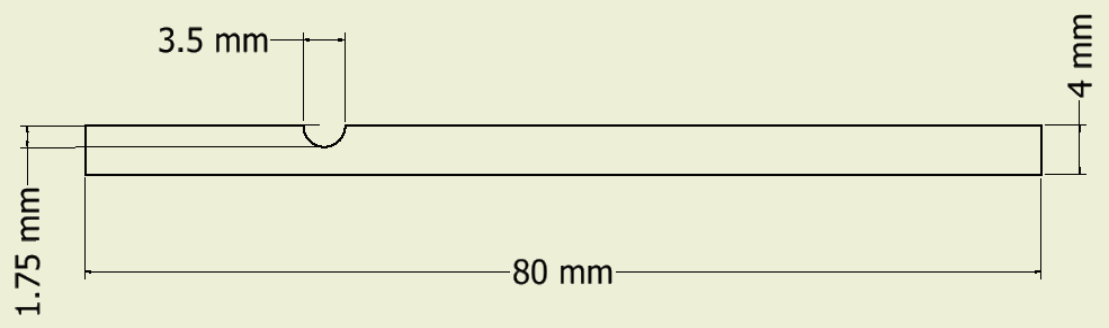


Figure 35. Technical drawing of pure iron core with notch

The valve is moved by linear actuator. In Figure 35 the notch on the valve can be seen easily. Thanks to that diameter change magnetic flux leaves the iron core and the secondary winding, which can be seen easily in Figure 34, catches that flux and produces voltage due to core displacement. This phenomenon is as same as Faraday's Law of induction.

Thanks to new design, secondary winding stays completely under the magnetic field which is generated by primary winding. However, due to design nature of this type of sensor, number of winding of primary winding is greater that the secondary winding. This is also efficient because of generating magnetic field. According to magnetic theory, if the number of winding increases, the generated magnetic field by solenoid will increases. To saturate the wall thickness of valve guide, this brings an advantage. Furthermore, this design brings efficiency. When the number of windings increase, adequate magnetic field can be generated by less power consumption. This can also be seen in Table 9.

The material properties and sensor properties are the same for three engine states, which are idling, running, and overspeeding, and given below.

- Number of windings of primary coil: 60
- Number of windings of secondary coil: 30
- Material of valve guide: Bronze
- Relative magnetic permeability of valve guide: 1.20
- Relative permeability of valve (pure iron): 100

The sensor behavior under different engine states is examined, from 4.3.1.1 to 4.3.1.3.

### 4.3.1.1. Engine at Idling State

All of the vehicles pass idling state after cranking. Nominal engine speed at idling is 600 rpm. When rpm converts into Hz, engine speed will be 5 Hz. Inlet or exhaust valve is opening and closing once upon 2 revolution. Which means valve is operating at 5 Hz when engine state at idling.

In Figure 36, blue signal is coming the output signal of the sensor while yellow signal is valve actuator signal. When electromagnetically actuated intake valve opens, the sensor gives an output signal as negative voltage. The reason is “Nature abhors magnetic field”. Peak to peak voltage is observed as 72 mV. The displacement of the valve is 400 μm. The maximum voltage that sensor produces is 40 mV without amplifier circuit. With simple mathematic, the sensor produces 1 mV as per 10 μm. If the SNR (Signal-to-noise ratio) is calculated;

$$SNR = 10\,log\left(\frac{Signal\ Amplitude}{Noise\ Amplitude}\right)^2 \tag{4.1}$$

$$SNR = 10\,log\left(\frac{72\ mV}{1\ mV}\right)^2$$

$$SNR = 34.4968\ dB$$

As a result of Eq.4.1, signal to noise ratio is between acceptable range for the sensors.

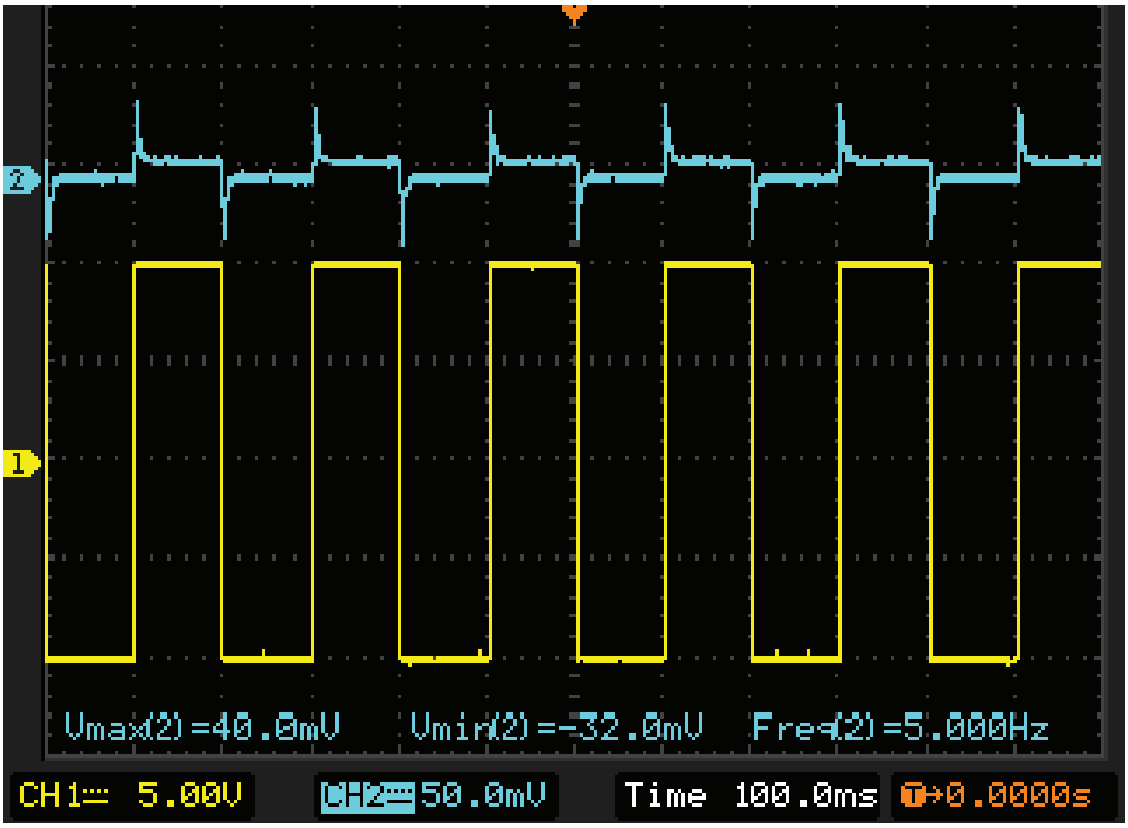


Figure 36. The output signal of the sensor at Engine state = IDLING

### 4.3.1.2. Engine at Running State

After idling state, engine passes to running state. If the engine is chosen as diesel engine, 1200 rpm will be the running state. When engine speed is 1200 rpm, intake valve is operating at 10 Hz.

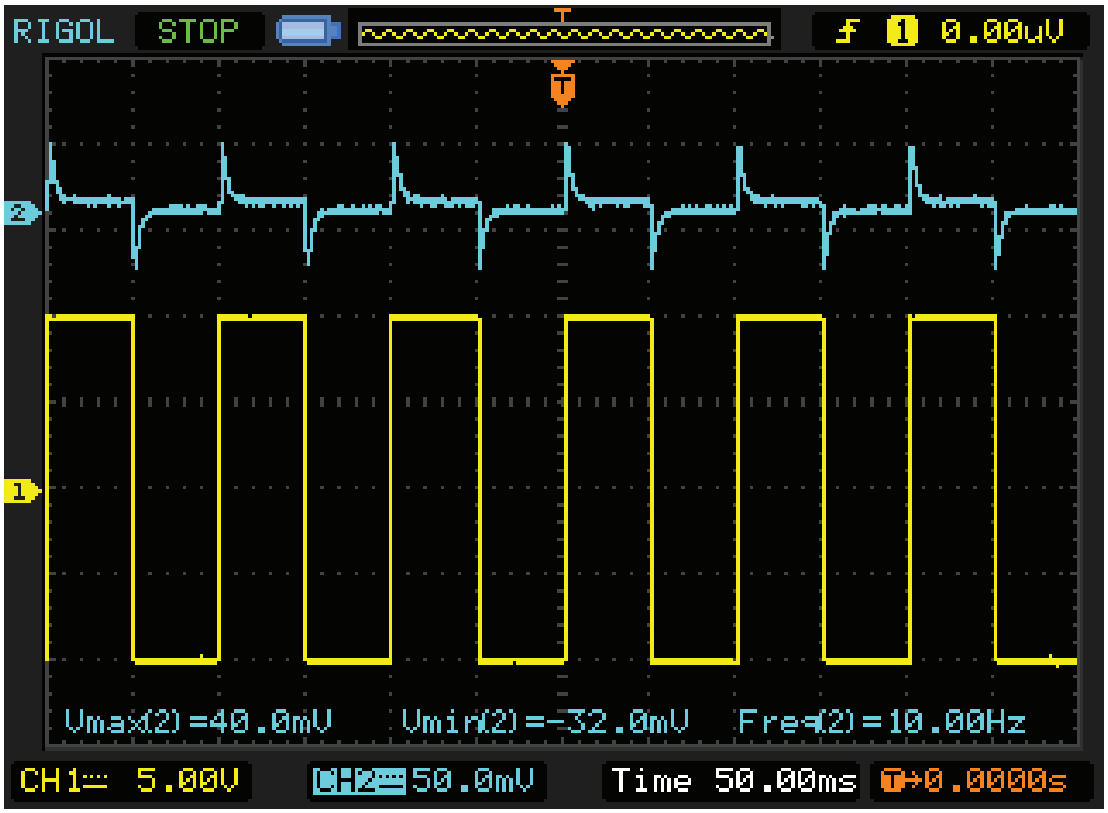


Figure 37. The output signal of the sensor at Engine state = RUNNING

In Figure 37, again total displacement of valve is 400 µm and result is the same. At running state of the engine, sensor still gives reliable information and correct results. The same signal to noise ratio is also valid for this engine speed and the state.

### 4.3.1.3. Engine at Overspeeding State

Overspeeding state is uncommon state for the vehicles. However, it does not mean that it never occurs. The operation range must be known for the sensors. Therefore, this state of engine is also considered.

In Figure 38, the amplitude of the signal, which is taken from the sensor output, has decreased compared with the previous state. This decreasing is because of experimental set up. Actuator cannot move 400 µm because of its mechanical limitations. In this state, the displacement of the valve is measured with the Vernier caliper, which has +/- 1 µm error, as 360 µm. However, in this state, signal to noise ratio is 32.1267 dB

which is less than idling and running states, but still between good (acceptable) ranges for the sensors.

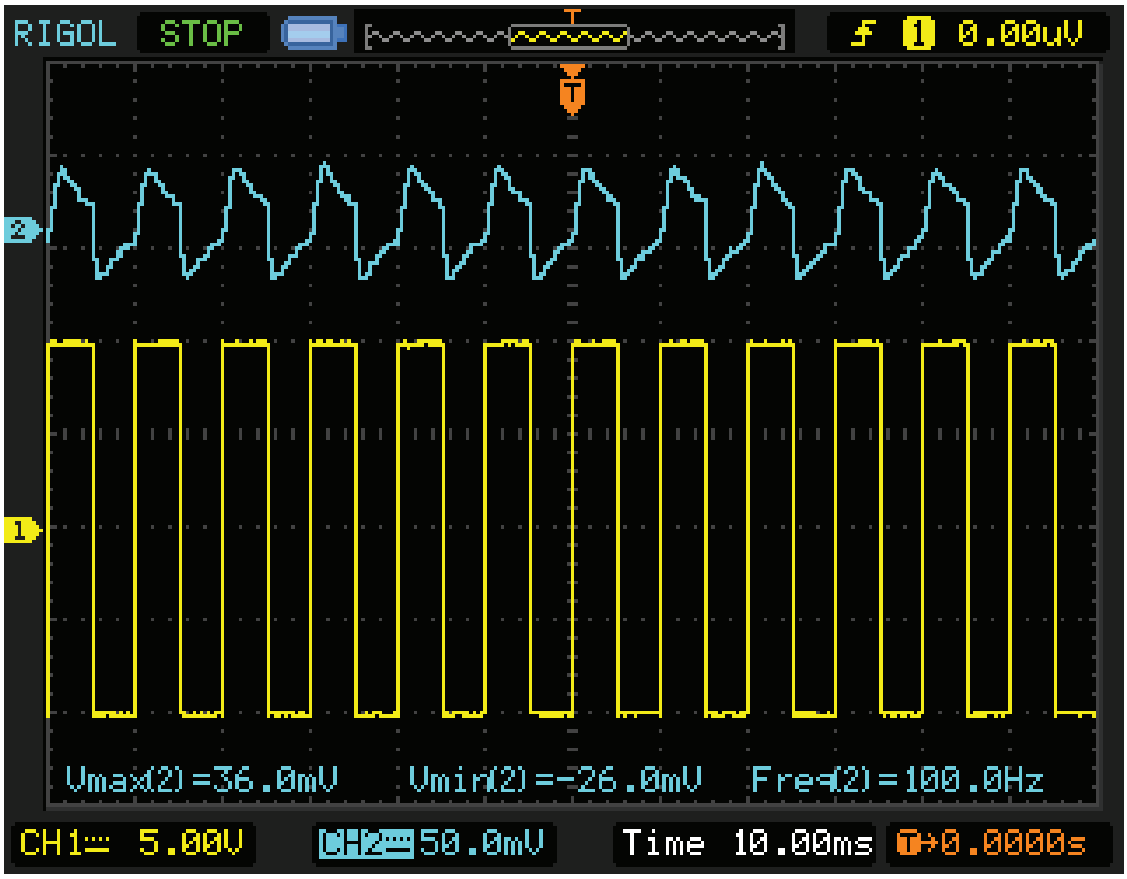


Figure 38. The output signal of the sensor at Engine state = OVERSPEEDING

The output signal is more likely to be sine wave instead of instantaneous peaks in overspeeding state. The reason is that the electromotive force increases, when the rate of change of the magnetic field is changing with respect to time. However, in this state, the sensor is exposed to saturation. This can be easily seen that the amplitude of the output signal is less than previous states.

# CHAPTER 5

# CONCLUSION

In recent decades there has been an increasing need and a push for mechanical systems in general to measure the sub-micron displacement changes. Although for some other engineering areas, such as electronics, this precision has been achieved earlier, it is still fairly new in mechanical engineering measurements. In many feedback control systems, precise displacement sensing is important. One of them, for the mechanical engineering, is the automotive industry. There are some dark areas which are known theoretically but not corroborated with real time data on road.

With this study, the problem of getting the valve displacement or injector needle displacement from the analog source is overcome. As discussed previously, displacement of intake and exhaust valves or needle of an SCR injector cannot be known from the data that is retrieved from an analog sensor source. They are mapped and estimated from experimental data. However, these estimations shall be poor because of driving style of the vehicle or usage of the system. The proposed sensor, Accuciser, with this study illuminates this area which is relatively dark place up to now. The study began with the LVDT sensor. However, LVDT is working with alternating current. In the engine or any type of injector, most of the parts are made of magnetic materials. Thus, alternating current has many drawbacks, such as skin effect.

After deep research, saturation phenomenon was found for the issues such as the current one. Magnetic saturation indicates that if the material is saturated with magnetic field lines, extra magnetic field line will effuse from the wall thickness of the material. The sensor was designed according to this phenomenon. It has two different coils and one coil is located on the top of the other. The outer coil is fed by direct current and this is one of the most powerful side which spare Accuciser from other types of displacement sensors, such as LVDT.

For an injector nozzle, the calculation was performed, and minimum required current was found to saturate the wall thickness for an example injector nozzle. The material is strengthened steel and its relative permeability was high. Therefore, calculated

minimum required current was relatively high for a sensor for automotive industry. On the other hand, this sensor can be used on HIL (Hardware in the Loop) environment.

Then, the sensor was mounted onto the valve guide. In the last decades, camless engines have become popular. Last but not the least, Koenigsegg company built the engine for a model named as Regera with camless, electromagnetically actuated free valve. These types of valves can be controlled easier than valve with camshaft. If Accuciser is mounted to this type of valves, it will not need a power supply to operate, thanks to Faraday's Law of Induction. The experiments were carried out with respect to electromagnetically actuated valves.

There have been three main experiment for intake or exhaust valves. These three experiments were carried out with respect to three engine states which are idling, running and overspeeding. As can be seen from the experiments, SNR ratios for those three states are between acceptable and reliable ranges for the sensors. Accuciser gives reliable and correct results, without amplifier circuit. The sensor gives 1 mV incrementing as per 10 µm. For the experiments, the displacement changing was specified as 400 µm. Although, in the overspeed case, the valve actuator cannot operate with both 100 Hz and 400 µm, the output signal gives 36 mV. After measuring the displacement in this state, the valve operates with 360 µm a displacement. Cross-check was done with a Vernier caliper which has 20 µm resolution with +/- 1 µm error.

All in all, Accuciser may be the solution to measure valve or injector needle displacement on the road. Using Accuciser will hopefully decrease the fuel consumption and increase the efficiency of the engine with closed loop control of valve timing.

# REFERENCES


Amirante, R., Catalano, L. A., & Coratella, C. (2013). A new optical sensor for the measurement of the displacement of the needle in a common rail injector. *SAE Technical Papers*, *6*(May 2014). https://doi.org/10.4271/2013-24-0146

Balanis, C. A. (2012). *ADVANCED ENGINEERING ELECTROMAGNETICS* (2nd ed.). Retrieved from http://www.ghbook.ir/index.php?name=های ر سانه و ف رهنگ ذ ویِ ن&option=com_dbook&task=readonline&book_id=13650&page=73&chkhashk=ED9C9491B4&Itemid=218&lang=fa&tmpl=component

Blejan, M., Ilie, I., & Drumea, A. (2016). SMART TRANSDUCER FOR SPEED AND POSITION. *International Conference on Hydraulics and Pneumatics - HERVEX*, 68–72. Baile Govora.

Cope, D., & Wright, A. (2006). Electromagnetic fully flexible valve actuator. *SAE Technical Papers*. https://doi.org/10.4271/2006-01-0044

Coppo, M., Dongiovanni, C., & Negri, C. (2007). A Linear optical sensor for measuring needle displacement in common-rail diesel injectors. *Sensors and Actuators, A: Physical*, *134*(2), 366–373. https://doi.org/10.1016/j.sna.2006.05.038

Dobkin, B., Hamburger, J., & Pei, C.-W. (2015). Chapter 487 – Precision LVDT signal conditioning using direct RMS to DC conversion. In *Analog Circuit Design*. https://doi.org/10.1016/B978-0-12-800001-4.00487-7

Drumea, A., Vasile, A., Comes, M., & Blejan, M. (2006). System on Chip Signal Conditioner for LVDT Sensors. *2006 1st Electronic Systemintegration Technology Conference*, 629–634. https://doi.org/10.1109/ESTC.2006.280070

Ewing, J. A. (1892). Magnetic Induction. *Scientific American*, *34*(881supp), 14084–14085. https://doi.org/10.1038/scientificamerican11191892-14084supp

Farden, J. (2003). *HANDBOOK OF MODERN SENSORS PHYSICS, DESIGNS, and APPLICATIONS* (3rd ed.). Retrieved from http://www.kelm.ftn.uns.ac.rs/literatura/si/pdf/HandbookOfModernSensorsPhysicsDesignAndApplications.pdf

Figliola, R. S., & Beasley, D. E. (2010). Theory and Design for Mechanical Measurements. In L. Ratts, A. Melhorn, & T. Kulesa (Eds.), *Theory and Design for Mechanical Measurements* (5th ed., Vol. 5). John Wiley & Sons, Inc.

Fizzics Organisation. (2015, October 3). *Youtube*. Retrieved from https://i.ytimg.com/vi/3NYg34_vy7k/maxresdefault.jpg

Gundersen, Y. (2009). *Free Valve Technology* (KTH Industrial Engineering and Management). Retrieved from http://kth.diva-portal.org/smash/get/diva2:542744/FULLTEXT01

Korkmaz, H., & Can, B. (2003). A thermal expansion measurement system using a high temperature unguided half bridge displacement transducer. *Proceedings of the 20th IEEE Instrumentation Technology Conference (Cat. No.03CH37412)*, *2*(May), 1633–1638. https://doi.org/10.1109/IMTC.2003.1208026

Masi, A., Danzeca, S., Losito, R., Peronnard, P., Secondo, R., & Spiezia, G. (2014). A high precision radiation-tolerant LVDT conditioning module. *Nuclear Instruments and Methods in Physics Research, Section A: Accelerators, Spectrometers, Detectors and Associated Equipment*, *745*(2014), 73–81. https://doi.org/10.1016/j.nima.2014.01.054

Osborne, R. J., Stokes, J., Lake, T. H., Carden, P. J., & Mullineux, J. D. (2018). *Development of a Two-Stroke / Four-Stroke Switching Gasoline Engine – The 2 / 4SIGHT Concept*. *2005*(724). https://doi.org/https://doi.org/10.4271/2005-01-1137

Popov, A. P., & Chugulev, A. O. (2012). A Study of a magnetic field for a sensor for detection of ferromagnetic bodies in the interior of a steel pipe. *Russian Electrical Engineering*, *83*(7), 404–406. https://doi.org/10.3103/S1068371212070103

Rathor, V. (2017, March 24). *Slide Share*. Retrieved from https://www.slideshare.net/vijendrarathor849/bh-curve-73581533

Sellnau, M., & Rask, E. (2003). Two-step variable valve actuation for fuel economy, emissions, and performance. *SAE Technical Papers*, *2003*(724). https://doi.org/10.4271/2003-01-0029

Suresh, C. V., & Ramu, G. (2012). *Real Time Measurement of Position as well as Direction using Linear Variable Differential Transformer*. *2*(3), 246–252.

Tanriyapisi, O. M., & Ozdemir, S. (2017). The Effect of Number of Coils and Diameter of Copper Wire on Output Signal of LVDT. *Imeset'17, International Conference on Multidisciplinary, Science, Engineering and Technology*, 1–7. Bitlis.

Ulaby, F. T., & Ravaioli, U. (2014). *Fundamentals Applied Electromagnitics* (7th ed.). Retrieved from http://em.groups.et.byu.net/embook/figs/figs9.html

Wikipedia. (2019, October 29). *Wikipedia*. Retrieved from https://en.wikipedia.org/wiki/Solenoid: https://en.wikipedia.org/wiki/Solenoid